Boundary conditions and behavior of the macroscopic fundamental diagram based network traffic dynamics: A control systems perspective

R. X. ZHONG [a], Y. P. HUANG [a], C. CHEN [a], W. H. K. LAM [b], D. B. XU [c], A. SUMALEE [b,*]

[a]*Guangdong Key Laboratory of Intelligent Transportation Systems, School of Engineering, Sun Yat-sen University, Guangzhou, China*
[b]*Department of Civil and Environmental Engineering, The Hong Kong Polytechnic University, Hong Kong SAR, China.*
[c]*School of Automation, Nanjing University of Science and Technology, Nanjing, China.*

Abstract

Macroscopic fundamental diagram (MFD), establishing a mapping from the network flow accumulation to the trip completion rate, has been widely used for aggregate modeling of urban traffic network dynamics. Based on the MFD framework, extensive research has been dedicated to devising perimeter control strategies to protect the network from gridlock. Recent research has revealed that the stochasticity and time-varying nature of travel demand can introduce significant scattering in the MFD, thus reducing the definition of the MFD dynamics. However, this type of demand effect on the behavior of the MFD dynamics has not been well studied. In this article, we investigate such effect and propose some appropriate boundary conditions to ensure that the MFD dynamics are well-defined. These boundary conditions can be regarded as travel demand adjustment in traffic rationing. For perimeter control design, a set of sufficient conditions that guarantee the controllability, an important but yet untouched issue, are derived for general multi-region MFD systems. The stability of the network equilibrium and convergence of the network dynamics are then analyzed in the sense of Lyapunov. Both theoretical and numerical results indicate that the network traffic converges to the desired uncongested equilibrium under proper boundary conditions in conjunction with proper control measures. The results are consistent with some existing studies and offer a control systems perspective regarding the demand-oriented behavior analysis of MFD-based network traffic dynamics. A surprising finding is that if the control purpose is to regulate the traffic to a desired level of service, the perimeter control gain can be simply chosen as its desired steady state, that is, the control gain is a constant and can be implemented as proportional control. This property sheds light on the road pricing design based on the MFD framework by minimizing the gap between the actual traffic state and the desired traffic state.

Keywords: Macroscopic fundamental diagram, boundary condition, feasible and admissible demand, stability and convergence, controllability.

*Corresponding author
E-mail addresses: zhrenxin@mail.sysu.edu.cn (R. X. ZHONG)., huangyp9@mail2.sysu.edu.cn (Y. P. HUANG)., chencan5@mail2.sysu.edu.cn (C. CHEN)., cehklam@polyu.edu.hk (W. H. K. LAM)., xu.dabo@gmail.com (D. B. XU)., asumalee@gmail.com (A. SUMALEE).

1. Introduction

Since Godfrey (1969) proposed the physical model of macroscopic fundamental diagrams (MFDs) and Daganzo (2007) proved its theoretical existence, MFDs have been widely investigated (see Haddad and Geroliminis, 2012; Haddad et al., 2013; Keyvan-Ekbatani et al., 2013; Leclercq et al., 2014; Yildirimoglu and Geroliminis, 2014; Leclercq et al., 2017; Saeedmanesh and Geroliminis, 2017, and the references therein). An MFD intuitively establishes a mapping from the network flow accumulation to the trip completion rate, providing an analytically simple and computationally efficient framework for aggregate modeling of urban traffic network dynamics. Under certain regularity conditions, such as stationary (or slow-varying) and distributed demand, and a homogeneous network infrastructure, well-defined MFDs were proven to exist for homogenous urban traffic networks by empirical and simulation studies (Geroliminis and Daganzo, 2008).

Extensive research has been dedicated to the development of various perimeter and gating control for traffic networks (see for example Haddad and Geroliminis, 2012; Aboudolas and Geroliminis, 2013; Geroliminis et al., 2013; Haddad and Shraiber, 2014; Haddad, 2015; Kouvelas et al., 2015, 2017). However, scatter in the network-wide flow-density relationship and hysteresis loops in MFD for higher densities were observed in both simulated and real networks by Mazloumian et al. (2010); Daganzo et al. (2011); Gayah and Daganzo (2011); Geroliminis and Sun (2011). For networks with spatial heterogeneity in congestion distribution, scattered MFDs (even with hysteresis loops) and even instability or gridlock of traffic networks could be induced. Some studies presumed that the major causes of scatters in MFDs comprise asymmetric OD and route choices (Geroliminis and Sun, 2011; Knoop et al., 2012; Geroliminis et al., 2013; Leclercq and Geroliminis, 2013). Daganzo et al. (2011) classified the randomness of turning movements as one major reason for the clockwise hysteresis phenomenon in MFDs, and higher turning rates are also implied to render capacity and jamming at lower densities than those observed in the MFDs.

Studies (see for example Gayah and Daganzo, 2011; Daganzo et al., 2011; Zhang et al., 2013) have shown that the stochasticity and time-varying nature of travel demand have strong effects on the scatter of the MFD and its shape (e.g., hysteresis phenomena) and can even render the traffic dynamics unstable. Daganzo et al. (2011) showed that slow-varying demand does not significantly affect the MFD shape, whilst fast-loading demand drives the network towards unstable equilibria and eventually a jam at higher densities. Gayah and Daganzo (2011) found that an MFD admits hysteresis loops even under the most favorable network conditions, if there are disturbances that cause randomness in route choices, such as unevenness during the late stages of a rush hour when more trips are terminating than starting, especially when drivers do not navigate through congestion in an adaptive manner. Zhang et al. (2013) found that for networks with time-independent boundary conditions, well-defined stationary MFDs can be observed, even if the demand is not uniform. The shape of the MFD depends on the level of heterogeneity in the system and the nature of the non-uniformity of demand. The MFDs achieve similar capacities in conjunction with high critical densities when the travel demand is uniformly distributed, whilst they display a steep drop in the flow just beyond the maximum of the MFD for networks that are subject to anisotropic exogenous demand. For time-dependent demand, MFDs show clear hysteresis that is strongly correlated with the spatial heterogeneity of the density. The qualitative behavior of this hysteresis is strongly dependent on the level of uniformity of boundary loading. To sum up, the theoretical MFD represents only steady-state behavior and holds only when the inputs change slowly in time and when traffic is distributed homogenously in space (Mahmassani et al., 2013). Furthermore, Geroliminis and Daganzo (2008); Mahmassani et al. (2013) claimed that the MFD can be determined only up to the maximum sustainable accumulation, rather than the jam accumulation (a complete standstill with zero flow). Gayah and Daganzo (2011) found that the flow-density relationship becomes more scattered at high densities via simulation of a symmetric two-ring

system.

Although the existence of an MFD and network stability is heavily affected by the demand pattern or boundary loading (denoted as 'boundary condition' hereafter), to the best knowledge of the authors, little research effort has been dedicated to analytic investigation of the interaction between the demand pattern (or boundary condition) and the network stability (and its subsequent controllability). As revealed by previous studies, to ensure a well-defined MFD, the network travel demand or boundary condition must fulfil certain conditions with respect to the network traffic state. In contrast, current research efforts tend to devise control strategies to guarantee network stability under arbitrary demand patterns. This is unnecessary or even impossible because stochastic or fast time-varying demand would introduce significant hysteresis to the MFD. Physically, given a traffic network and its MFD, the maximum throughput (or capacity) of the network is a known finite value. Not all travel demand can be loaded onto the road network, but the capacity is saturated at any given moment.

The theory of MFD has its root in the kinematic wave theory (Daganzo, 2007; Jin et al., 2013). A popular numerical scheme of the kinematic wave model is the cell transmission model (CTM). Regarding boundary conditions [1], the original CTM assumes that the boundaries of a freeway segment can always receive and discharge vehicles at either the maximum allowed speed (or free flow speed) or the maximum allowed flow rate (or capacity). However, in an actual freeway segment, traffic at the boundaries may be either free-flowing or congested at different times of day. Proper boundary conditions have been deemed necessary to enable the model to work with real data for traffic simulation and advanced control purposes (Muñoz et al., 2004; Zhong et al., 2016a,b). Gomes et al. (2008) analyzed the CTM, including the structure of its equilibrium points, their stability, and the convergence of its trajectories, under stationary demand and proper boundary conditions. They found that the equilibrium behavior depends on the pattern of demand. One surprising conclusion of their analysis was that depending on the initial conditions, the same demand may leave a segment uncongested or it may congest one or more sections, or even the entire segment. To secure the existence of equilibrium and its stability, a (strictly) feasible stationary demand concept was proposed. Geng et al. (2015) proposed demand adjustment strategies that redistribute the stationary feasible demand so that the network state can converge to uncongested equilibria after demand adjustment. Jin et al. (2013) showed that all stationary states in the MFD are stable and can be reached using the simulation results from a corresponding CTM for the double-ring network under constant demand. Jin et al. (2013) stated that understanding stationary and dynamic traffic patterns in general road networks under the MFD framework is an emerging but much more challenging task.

Along this stream, most existing works in the MFD literature, e.g., Haddad and Geroliminis (2012); Haddad and Shraiber (2014) investigated the stability issue without considering the effects of the boundary conditions. On the other hand, Ramezani et al. (2015) considered the effect of receiving capacity, which can be regarded as a special case of boundary condition, without addressing the stability. Comparing this paper with a closely related research (Haddad and Geroliminis, 2012) helps identifying the contribution. The key similarities and distinctions are summarized in Table 1. The stability analysis in Haddad and Geroliminis (2012) concentrates on two-region MFD system with single-direction perimeter control. Local stability around the reference point to which the linearization is performed was deduced from eigenvalue analysis of the system matrix obtained from Jacobian linearization of the MFD system. Thus, it is necessary to acquire the region of attraction (ROA). It is well known that estimating the region of attraction is generally impossible (Khalil, 2002; Haddad and Chellaboina, 2008). Distinguished from the local stability analysis, our objective is to realize a global stability analysis that covers the whole feasible region of general

---

[1] In the CTM, flows entering and exiting freeway boundaries are regarded as demand patterns or disturbances.

3

multi-region MFD systems. Moreover, this article addresses another important but yet untouched issue for perimeter control design, i.e., the controllability for general multi-region MFD systems.

Table 1: A comparison among Haddad and Geroliminis (2012), Zhong et al. (2017) and this article

	Haddad and Geroliminis (2012)	Zhong et al. (2017)	This article
MFD dynamics	Two-region with single-direction perimeter control	Two-region with two-direction perimeter control	General multi-region (includes single-region, two-region and three-region as special cases)
Control input	Single-input (single control variable)	Two-input (a vector of control variables)	Multi-input (a vector of control variables)
MFD shape	Triangular (trapezoidal MFDs are studied in numerical examples)	Unimodal right-skewed	Unimodal right-skewed
Demand pattern	Constant	Constant & time-varying	Constant & time-varying
Linearization	✓	✗	✗
Methodology	Eigenvalue analysis of the linearized system	Control-Lyapunov function	Lyapunov theory
Existence of steady state	✗	Necessary conditions for two-region MFD system	Necessary conditions for general multi-region MFD systems
Stability	Local (the ROA is related to the initial condition & triangular MFD)	Global (independent of the functional form of the MFD)	Global (independent of the functional form of the MFD)
Controllability	✗	Sufficient conditions for two-region MFD system	Sufficient conditions for general multi-region MFD systems
Boundary condition	✗	✓	✓
Controller design	Bang-bang like optimal control	Bang-bang like and almost smooth robust control	Proportional control

In light of the above discussion, this paper aims to devise some appropriate boundary conditions for travel demand adjustment to ensure the well posedness of MFD dynamics even under time-varying demand. Furthermore, another key motivation is to devise a set of sufficient conditions that guarantee the controllability (to be more specific, stabilizability), an important but yet untouched issue, for general multi-region MFD systems, so that the desired network state can be achieved by perimeter/gating control. By applying the boundary conditions proposed in the paper, Zhong et al. (2017) managed to establish two universal robust dynamic perimeter controllers that globally stabilize the two-region MFD system with inherent demand and MFD parametric uncertainties. The similarities and distinctions with Zhong et al. (2017) which distinguish the contribution of this paper are summarized in Table 1. While Zhong et al. (2017) concentrates on the robust controller design for two-region MFD systems, the key message delivered by the analysis in this paper is that any perimeter control that can regulate the traffic state to the target equilibrium has to converge to the corresponding steady state obtained from the steady-state equations. If there is no other effective method or the traffic manager is lack of comprehensive controller tuning skill, the perimeter control gain can be simply chosen as its desired steady state.

The rest of the paper is organized as follows. Section 2 presents the traffic dynamics of general multi-region MFD system while includes single-region and two-region as special cases in line with the literature. Some modifications are then introduced to refine the MFD system(s) in light of the CTM. Section 3 introduces the feasible demand concept and derives necessary conditions for the existence of equilibrium with respect to a given travel demand pattern. With the help of admissible travel demand, the stability of the

network equilibrium and convergence of the network dynamics are then analyzed in Section 4 in the sense of Lyapunov, wherein a set of sufficient conditions for controllability by perimeter or gating control are also derived. The simulation results are presented in Section 5 to demonstrate the theoretical development. Finally, conclusions are drawn and future works are outlined in Section 6. For a better grasp and understanding of this paper, a precedence diagram for analysis of the stability of the equilibrium and convergence of system dynamics and Table 2 collecting key variables throughout this paper are provided below.
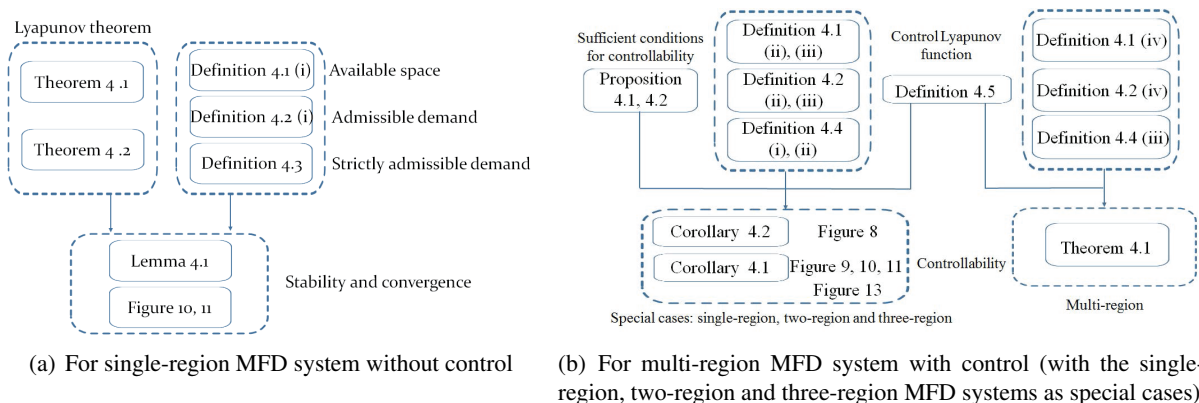

(a) For single-region MFD system without control

(b) For multi-region MFD system with control (with the single-region, two-region and three-region MFD systems as special cases)

Figure 1: Precedence diagram for stability, convergence and controllability of the MFD systems

Table 2: List of key notations

Symbol	Meaning
$n_{ii}(t)$	Number of vehicles in R_i with destination inside the region at time t
$n_{ij}(t)$	Number of vehicles in R_i with destination to R_j at time t
$n_i(t)$	Accumulation or total number of vehicles in R_i at time t, and $n_i = n_{ii}(t) + \sum_j n_{ij}(t)$
$G_i(n_i(t))$	MFD that maps the network accumulation $n_i(t)$ to trip completion rate for region i at time t
$q_{ii}(t)$	Endogenous travel demand whose origin and destination are in the same region i
$q_{ij}(t)$	Exogenous travel demand whose origin i and destination j are not in the same region, i.e., $i \neq j$
$\tilde{q}_i$	strictly admissible demand which generates from R_i
$u_{ij}(t)$	Perimeter controllers controlling the ratio of the transfer flow that transfer from R_i to R_j at time t
$\bar{n}_i^s$	stable equilibrium which lies in the left side of $n_{i,cr}$
$\bar{n}_i^u$	unstable equilibrium which lies in the right side of $n_{i,cr}$
$\bar{n}_i$	the steady state of accumulation n_i
$\bar{q}_i$	the steady state of travel demand of q_i
$\bar{u}_{ij}$	the steady state of perimeter control u_{ij}

2. MFD system dynamics and its modification

MFDs are widely used for aggregated network traffic modeling and control for networks with homogeneously distributed traffic and stationary (or slow-varying) travel demand. It is assumed that all trips within the region, whether internal or external, share a similar trip length, that is, the distance traveled per vehicle depends upon neither its origin nor its destination. Denote $n_i(t)$ as the regional traffic accumulation or the

5

total number of vehicles in the region i at time t; a concave function of $n_i(t)$, denoted by $G_i(n_i(t))$ and termed as the MFD, is defined as the trip completion flow for region i when network traffic state is $n_i(t)$ (see for example Geroliminis et al., 2013; Haddad, 2015).

2.1. Multi-region MFD system

A heterogeneous urban network decomposed into L homogeneous subregions wherein each region admits a well-defined MFD is considered in line with Haddad (2015). Endogenous travel demand is defined as a flow whose origin and destination are within the same region, whereas the origin and destination of exogenous travel demand are not the same. Let $q_{ij}(t)$ (veh/s) denote the traffic flow demand generated in region i with direct destination to region j, where $i = 1, \ldots, L$, $j \in S_i$, and S_i denotes the set of the subregions directly connected to subregion i. By definition, each S_i is a set of integers corresponding to the index number of regions. The dynamic system states (accumulations) are defined based on flow conservation according to destination oriented traffic demand as: $n_{ii}(t)$ (veh) is the total number of vehicles in region i with destination inside the region; $n_{ij}(t)$ (veh) is the number of vehicles in region i with direct destination to region j. Accumulation or the total number of vehicles in region i is thus evaluated as $n_i(t) = n_{ii}(t) + \sum_{j \in S_i} n_{ij}(t)$.

The trip completion flow for region i is the sum of transfer flows, i.e., trips from region i with destination in region j, $j \in S_i$, plus the internal flow, i.e., trips from i with destination inside the region. The transfer flow from region i with destination to region j is calculated corresponding to the fraction between accumulations, i.e., $n_{ij}(t)/n_i(t)G_i(n_i(t))$, and the internal flow from region i with destination inside the region is also calculated corresponding to the fraction between accumulations, i.e., $n_{ii}(t)/n_i(t)G_i(n_i(t))$. The dynamic vehicle-conservation equations of the L-region MFD system are then formulated as follows:

$$\frac{\mathrm{d}n_{ii}(t)}{\mathrm{d}t} = -\frac{n_{ii}(t)}{n_i(t)}G_i(n_i(t)) + \sum_{j \in S_i} \frac{n_{ji}(t)}{n_j(t)}G_j(n_j(t))u_{ji}(t) + q_{ii}(t) \tag{1a}$$

$$\frac{\mathrm{d}n_{ij}(t)}{\mathrm{d}t} = -\frac{n_{ij}(t)}{n_i(t)}G_i(n_i(t))u_{ij}(t) + q_{ij}(t) \tag{1b}$$

$$n_i(t) = n_{ii}(t) + \sum_{j \in S_i} n_{ij}(t) \tag{1c}$$

subject to $0 \le u_{\min} \le u_{ij}(t) \le u_{\max} \le 1$, $0 \le u_{\min} \le u_{ji}(t) \le u_{\max} \le 1$, where $i = 1, \ldots, L$, $j \in S_i$. $u_{ij}(t)$ and $u_{ji}(t)$, $i = 1, \ldots, L$, $j \in S_i$, denote the perimeter control inputs, which are introduced on the border between the regions i and j, to control the transfer flows between the regions. The cross-boundary flow $n_{ij}(t)/n_i(t)G_i(n_i(t))$, $i = 1, \ldots, L$, $j \in S_i$, is controlled such that only a fraction of the flow actually transfers from region i to region j, i.e., $n_{ij}(t)/n_i(t)G_i(n_i(t))u_{ij}(t)$. Summing (1a) and (1b), and denoting $v_{ii}(t) = \frac{n_{ii}(t)}{n_i(t)}$, $v_{ij}(t) = \frac{n_{ij}(t)}{n_i(t)}$, $q_i(t) = q_{ii}(t) + \sum_{j \in S_i} q_{ij}(t)$, for $i = 1, \ldots, L$, $j \in S_i$, one gets

$$
\begin{aligned}
\frac{\mathrm{d}n_i}{\mathrm{d}t} &= q_i - v_{ii}G_i(n_i) - \sum_{j \in S_i} v_{ij}G_i(n_i) \cdot u_{ij} + \sum_{j \in S_i} v_{ji}G_j(n_j) \cdot u_{ji} \\
&= q_i - G_i(n_i) + (1 - v_{ii})G_i(n_i) - \sum_{j \in S_i} v_{ij}G_i(n_i) \cdot u_{ij} + \sum_{j \in S_i} v_{ji}G_j(n_j) \cdot u_{ji} \\
&= q_i - G_i(n_i) + \sum_{j \in S_i} v_{ij}G_i(n_i) - \sum_{j \in S_i} v_{ij}G_i(n_i) \cdot u_{ij} + \sum_{j \in S_i} v_{ji}G_j(n_j) \cdot u_{ji} \\
&= q_i - \left[G_i(n_i) - \sum_{j \in S_i} v_{ij}G_i(n_i) \cdot (1 - u_{ij}) - \sum_{j \in S_i} v_{ji}G_j(n_j) \cdot u_{ji} \right]
\end{aligned} \tag{2}
$$

Two important special cases are frequently investigated in the literature, i.e., the single-region MFD system and the two-region MFD system.

2.2. Single-region MFD system

In line with Haddad and Shraiber (2014), a homogeneous urban region with three ODs and perimeter controllers is considered. $q_{11}(t)$ (veh/s) is the travel demand with both the origin and the destination in the region; $q_{12}(t)$ (veh/s) is the travel demand with the origin in the region and the destination outside the region; and $q_{21}(t)$ (veh/s) is the travel demand with the origin outside the region and the destination in the region. All other state and control variables share the same meanings as those of the multi-region case. Perimeter controller on the border with coupled inputs $u(t)$ and $1 - u(t)$, $0 \leq u(t) \leq 1$ [2] is introduced to control the cross-boundary traffic flow, wherein $1 - u(t)$, $u(t)$ denote the ratio of the transfer flows entering and exiting the protected region, respectively. Therefore, the vehicle-conservation equations are given as follows

$$\frac{dn_{11}(t)}{dt} = q_{11}(t) + (1 - u(t))q_{21}(t) - \frac{n_{11}(t)}{n_1(t)}G_1(n_1(t)) \tag{3a}$$

$$\frac{dn_{12}(t)}{dt} = q_{12}(t) - \frac{n_{12}(t)}{n_1(t)}G_1(n_1(t))u(t) \tag{3b}$$

Similar to the multi-region case, let $q_1(t) = q_{11}(t) + q_{12}(t)$, $n_1(t) = n_{11}(t) + n_{12}(t)$, and $\upsilon(t) = \frac{n_{11}(t)}{n_1(t)}$. Summing (3a) and (3b), one gets

$$\frac{dn_1(t)}{dt} = q_1(t) + q_{21}(t) - \upsilon(t)G_1(n_1(t)) - \left[q_{21}(t) + (1 - \upsilon(t))G_1(n_1(t))\right]u(t) \tag{4}$$

subject to $0 \leq n_1(t) < n_1^{jam}$, $0 \leq u_{\min} \leq u(t) \leq u_{\max} \leq 1$. Here, $n_{11}(t_0) = n_{11}(0)$ and $n_{12}(t_0) = n_{12}(0)$ are the initial accumulations at t_0, n_1^{jam} is the jam accumulation of the region, and $u_{\min}$ and $u_{\max}$ are the lower and upper bounds for $u(t)$.

In particular, the simplest case is a single-region MFD system without external traffic, whose dynamics can be simplified as

$$\frac{dn(t)}{dt} = q(t) - G(n(t)) \tag{5}$$

where $q(t)$ is the travel demand within the region. $n(t)$ denotes the region accumulation or the total number of vehicles in the region at time t, and $G(n(t))$ is the corresponding trip completion flow.

2.3. Two-region MFD system

An urban traffic network that can be partitioned into two homogeneous sub-networks wherein each region admits a well-defined MFD is considered in line with Haddad and Geroliminis (2012); Geroliminis et al. (2013). For the two-region system, there are two endogenous travel demands, i.e., q_{11} (veh/s) in region 1, and $q_{22}(t)$ (veh/s) in region 2, and two exogenous travel demands, i.e., $q_{12}(t)$ (veh/s) and $q_{21}(t)$ (veh/s),

---

respectively. Corresponding to the endogenous and exogenous travel demands, four accumulation states are used to describe the system dynamics in the literature.

$$\frac{\mathrm{d}n_{11}(t)}{\mathrm{d}t} = -\frac{n_{11}(t)}{n_1(t)}G_1(n_1(t)) + \frac{n_{21}(t)}{n_2(t)}G_2(n_2(t))u_{21}(t) + q_{11}(t) \tag{6a}$$

$$\frac{\mathrm{d}n_{12}(t)}{\mathrm{d}t} = -\frac{n_{12}(t)}{n_1(t)}G_1(n_1(t))u_{12}(t) + q_{12}(t) \tag{6b}$$

$$\frac{\mathrm{d}n_{21}(t)}{\mathrm{d}t} = -\frac{n_{21}(t)}{n_2(t)}G_2(n_2(t))u_{21}(t) + q_{21}(t) \tag{6c}$$

$$\frac{\mathrm{d}n_{22}(t)}{\mathrm{d}t} = -\frac{n_{22}(t)}{n_2(t)}G_2(n_2(t)) + \frac{n_{12}(t)}{n_1(t)}G_1(n_1(t))u_{12}(t) + q_{22}(t) \tag{6d}$$

subject to

$$0 \leq n_{11}(t) + n_{12}(t) < n_1^{jam}, \quad 0 \leq n_{21}(t) + n_{22}(t) < n_2^{jam} \tag{7a}$$

$$0 \leq u_{\min} \leq u_{12}(t) \leq u_{\max} \leq 1, \quad 0 \leq u_{\min} \leq u_{21}(t) \leq u_{\max} \leq 1 \tag{7b}$$

Here, $n_1(t) = n_{11}(t) + n_{12}(t)$, $n_2(t) = n_{21}(t) + n_{22}(t)$, $n_{11}(t_0) = n_{11}(0)$, $n_{12}(t_0) = n_{12}(0)$, $n_{21}(t_0) = n_{21}(0)$, $n_{22}(t_0) = n_{22}(0)$, where $n_{ij}(0), i, j = 1, 2$ are the initial accumulation at t_0. n_1^{jam} and n_2^{jam} (veh) are jam accumulations of region 1 and 2, respectively. $u_{\min}$ and $u_{\max}$ are the lower and upper bounds for $u_{12}(t)$ and $u_{21}(t)$, respectively. Summing (6a) and (6b), (6c) and (6d), respectively, and denoting $v_{ii}(t) = \frac{n_{ii}(t)}{n_i(t)}$, $v_{ij}(t) = \frac{n_{ij}(t)}{n_i(t)}$, $q_i(t) = q_{ii}(t) + q_{ij}(t)$, for $i, j = 1, 2$, one obtains the two-state two-region MFDs dynamics in line with Haddad (2015) as:

$$\frac{\mathrm{d}n_1(t)}{\mathrm{d}t} = -v_{11}(t)G_1(n_1(t)) - v_{12}(t)G_1(n_1(t))u_{12}(t) + v_{21}(t)G_2(n_2(t))u_{21}(t) + q_1(t) \tag{8a}$$

$$\frac{\mathrm{d}n_2(t)}{\mathrm{d}t} = -v_{22}(t)G_2(n_2(t)) - v_{21}(t)G_2(n_2(t))u_{21}(t) + v_{12}(t)G_1(n_1(t))u_{12}(t) + q_2(t) \tag{8b}$$

subject to the same constraints on state and control variables described in (7a)-(7b), and $v_{11}(t) + v_{12}(t) = 1$, $v_{21}(t) + v_{22}(t) = 1$, $v_{11}(t_0) = v_{11}(0)$, $v_{12}(t_0) = v_{12}(0)$, where $v_{ij}(0), i, j = 1, 2$, are the initial ratios of accumulation at t_0.

2.4. Modifications to the MFD system

Similar to the CTM, a sink is connected to each region to store all traffic that completes the trip. In contrast, given a traffic network and its MFD, the maximum throughput (or capacity) of the network is a known finite value for which not all travel demand can enter the network, which is saturated by its capacity at any given moment. Thus, a source is introduced to hold the demand that cannot enter the network. For illustration, the modified single-region and two-region MFD systems are respectively depicted in Figure 2(a) and Figure 2(b), where $\tilde{q}_i$ denotes the travel demand satisfying a set of boundary conditions for region i, which will be specified in the forthcoming sections.

(a) Modified single-region MFD system.
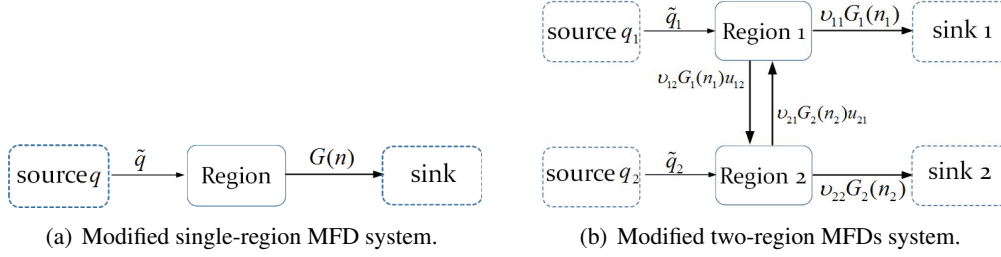
(b) Modified two-region MFDs system.

Figure 2: Modified MFD framework.

3. Steady-state equations and necessary conditions for solvability

Understanding the manner in which travel demand affects the existence of equilibrium to the MFD system, its stability and the controllability of the MFD systems can help to devise appropriate boundary conditions for travel demand adjustment and controller design to protect the network from gridlock. As reported in the literature that, for time-varying demand pattern that admits a steady state, the system might become gridlock when the demand is too high or if the demand is varying too rapidly. Even for the low demand case, gridlock is still likely to occur as long as the initial state is too congested. As we will see later, equilibrium might not exist if the demand is too high. This has been shown in Haddad and Geroliminis (2012) for the stationary demand case wherein the stability of two-region MFD system with constant demand is investigated via evaluating the eigenvalues of the system matrix of the linearized MFD system. However, linearization can only look into the local stability. Both calibrating the initial network state and estimating the region of attraction of the equilibrium of the linearized MFD system are difficult. To avoid the hurdle caused by linearization and to extend the analysis to time-varying demand case, we adopt a Lyapunov theory framework. The analysis begins with the simplest single region MFD system and is then generalized to the two-region and multi-region cases under both constant and time-varying demand patterns. To begin with, we derive necessary conditions for the existence of equilibrium with respect to a given travel demand pattern.

A point is said to be an equilibrium or a steady state of a dynamic system if, whenever the state starts from the point, the state will remain at the point for all future time (Khalil, 2002). Thus, we say that the MFD system is in equilibrium state if the accumulation state is invariant with time. Therefore, in equilibrium state, it holds that the derivatives of the state variables are equal to zero.

Denote $\bar{n}$ as an equilibrium induced by a known steady state of the travel demand $\bar{q}$, and let $G^{\max}$ be the maximal trip completion rate, that is, the network capacity. We start with the single-region MFD system without control, i.e., (5). Let $dn/dt = 0$, one gets $\bar{q} = G(\bar{n})$. The remaining deduction of the equilibrium for system (5) is trivial. Regarding the single-region system with control (3a)-(3b), let $dn_{11}/dt = 0$ and $dn_{12}/dt = 0$, one obtains

$$\bar{q}_{11} + (1 - \bar{u})\bar{q}_{21} = \frac{\bar{n}_{11}}{\bar{n}_1} G_1(\bar{n}_1), \quad \bar{q}_{12} = \frac{\bar{n}_{12}}{\bar{n}_1} G_1(\bar{n}_1)\bar{u}, \quad \bar{n}_1 = \bar{n}_{11} + \bar{n}_{12}$$

Readers can refer to Appendix A.1 or Haddad and Shraiber (2014) for the calculation of the steady states of the state variable $\bar{n}_{11}, \bar{n}_{12}$ and the control input $\bar{u}$.

For the two-region MFD system with control (6a)-(6d), let $\bar{n} = [\bar{n}_{11}, \bar{n}_{12}, \bar{n}_{21}, \bar{n}_{22}]^T$, $\bar{u} = [\bar{u}_{12}, \bar{u}_{21}]^T$ and $\bar{q} = [\bar{q}_{11}, \bar{q}_{12}, \bar{q}_{21}, \bar{q}_{22}]^T$ denote the steady states of the accumulation, controller and travel demand, respectively. Assume that the steady-state accumulation in each region ($\bar{n}_1$ and $\bar{n}_2$) is determined by a known

9

aggregated steady-state demand generated from each region ($\bar{q}_1$ and $\bar{q}_2$) as well as the control objective. Let $dn_{11}/dt = 0$, $dn_{12}/dt = 0$, $dn_{21}/dt = 0$ and $dn_{22}/dt = 0$, then $\bar{n} = [\bar{n}_{11}, \bar{n}_{12}, \bar{n}_{21}, \bar{n}_{22}]^T$ and $\bar{u} = [\bar{u}_{12}, \bar{u}_{21}]^T$ are calculated by solving the following steady-state equations:

$$0 = -\frac{\bar{n}_{11}}{\bar{n}_1}G_1(\bar{n}_1) + \frac{\bar{n}_{21}}{\bar{n}_2}G_2(\bar{n}_2)\bar{u}_{21} + \bar{q}_{11}, \quad 0 = -\frac{\bar{n}_{12}}{\bar{n}_1}G_1(\bar{n}_1)\bar{u}_{12} + \bar{q}_{12}, \quad \bar{n}_1 = \bar{n}_{11} + \bar{n}_{12}$$

$$0 = -\frac{\bar{n}_{22}}{\bar{n}_2}G_2(\bar{n}_2) + \frac{\bar{n}_{12}}{\bar{n}_1}G_1(\bar{n}_1)\bar{u}_{12} + \bar{q}_{22}, \quad 0 = -\frac{\bar{n}_{21}}{\bar{n}_2}G_2(\bar{n}_2)\bar{u}_{21} + \bar{q}_{21}, \quad \bar{n}_2 = \bar{n}_{21} + \bar{n}_{22}$$

More details are presented in Appendix A.2.

The steady-state equations of the multi-region MFD system can be similarly obtained which are omitted for brevity. Interested readers can refer to Appendix A.3 for the details.

Although we have derived a set of steady-state equations, their solvability is yet unclear. Thus, we derive the necessary conditions to guarantee that the above steady-state equations are solvable by following Haddad and Shraiber (2014).

Proposition 3.1. Under zero-initial condition, necessary conditions for the solvability of the steady-state equations are:
(i) For the single-region MFD system without control (5):

$$\bar{q} \leq G^{\text{max}}$$

(ii) Regarding the single-region MFD system with perimeter control (3a)-(3b):

$$\bar{q}_{11} + \bar{q}_{12} \leq G_1(\bar{n}_1)$$

(iii) Regarding the four-state two-region MFD system with perimeter control (6a)-(6d):

$$\bar{q}_{11} + \bar{q}_{12} + \bar{q}_{21} \leq G_1(\bar{n}_1), \quad \bar{q}_{22} + \bar{q}_{21} + \bar{q}_{12} \leq G_2(\bar{n}_2)$$

(iv) Regarding the multi-region MFD system with perimeter control (1a)-(1b):

$$\bar{q}_{ii} + \sum_{j \in S_i} \bar{q}_{ij} + \sum_{j \in S_i} \bar{q}_{ji} \leq G_i(\bar{n}_i)$$

A demand pattern is said to be feasible if its steady state can induce at least a feasible solution to the steady-state equations. ∎

PROOF OF PROPOSITION 3.1. Refer to Appendix A.4. ∎

Theorem 3.1. A feasible constant demand $\bar{q}$ induces two equilibria denoted by $\bar{n}^s$ and $\bar{n}^u$ for the single-region MFD system without control (5), where $0 \leq \bar{n}^s \leq n_{cr} \leq \bar{n}^u < n_{jam}$, with $\bar{n}^s$ and $\bar{n}^u$ denoting the uncongested equilibrium and congested equilibrium respectively. ∎

PROOF OF THEOREM 3.1. It holds that the derivative of n equals zero during the steady-state period. For the single-region MFD system, it is $0 = q - G(n)$; then two equilibria denoted $\bar{n}^s$ ($\bar{n}^s \leq n_{cr}$), $\bar{n}^u$ ($\bar{n}^u \geq n_{cr}$), respectively, can be derived by MFD mapping (see Figure 3). ∎
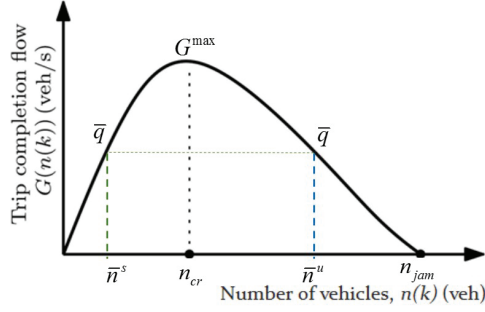
Figure 3: The relationship between the steady state of the demand and the MFD.

Intuitively speaking, Proposition 3.1 states that the steady state of the demand cannot exceed the maximum trip completion flow, that is, the capacity of the network $G^{\max}$ (see for example Figure 3). Otherwise, the steady-state equations are not solvable. As depicted in Figure 3 and shown in the Appendix, if the MFD is well-defined and if the steady-state equations are solvable, there will be two equilibria corresponding to the steady state of the demand and the concave shape of the MFD. We say that the equilibrium is stable if the system state can return or converge to it or to its neighborhood after any perturbations to the accumulation state (Daganzo et al., 2011). As it will be shown in the forthcoming section, $\bar{n}^s$ in the non-congested region of the MFD is a stable equilibrium whilst the other in the congested region of the MFD is an unstable equilibrium, similar to the CTM case by Gomes et al. (2008). To this end, $\bar{n}^s$ in the non-congested region of the MFD is more likely to be the desired steady state for the sake of urban mobility.

4. Admissible travel demand, stability and controllability

4.1. Admissible travel demand

As previously discussed, demand that exceeds the capacity could not be received by the network. Similar to the CTM, a set of demand-supply reaction laws must be devised to propagate traffic flow. A set of boundary conditions, denoted by admissible travel demand, that describe the demand-supply reaction laws under the MFD framework are proposed for both constant and time-varying travel demand patterns.

Definition 4.1. (**Admissible travel demand**) (i) For a single-region MFD system without control, i.e., (5), the **admissible travel demand** $\tilde{q}(t)$ can be defined as

$$\tilde{q}(t) = \begin{cases} \min\{q(t), G^{\max}\}, & 0 < n(t) \leq n_{cr} \\ \min\{q(t), G(n(t))\}, & n_{cr} < n(t) < n_{jam} \end{cases} \tag{9}$$

In particular, $q(t) \equiv \bar{q}$ for the constant demand case.

(ii) For a single-region MFD system with control, i.e., (3a)-(3b), the **admissible travel demand** $\tilde{q}(t)$ with given control can be defined as

$$\tilde{q}(t) = \min\left\{q(t), G_1(n_1(t)) - \left[q_{21}(t) + (1 - \upsilon(t))G_1(n_1(t))\right]\left(1 - u(t)\right)\right\}$$

where $q(t) = q_{11}(t) + q_{12}(t)$. $G_1(n_1(t))$ is the trip completion flow of the protected region at time t, i.e., the total available space, $q_{21}(t)(1 - u(t))$ is the cross-boundary demand would like to enter the protected region,

11

and $(1 - v(t)) \, G_1(n_1(t)) \, (1 - u(t))$ is the remaining transfer flow that would like to exit the protected region. In particular, $q(t) \equiv \bar{q} = \bar{q}_{11} + \bar{q}_{12}$ for the constant demand case.

(iii) For a two-region MFD system with control, i.e., (8a)-(8b), the **admissible travel demand** $\tilde{q}_i(t)$ with given control for Region i can be defined as

$$\tilde{q}_i(t) = \min\Big\{ q_i(t), G_i(n_i(t)) - v_{ji}(t) \, G_j(n_j(t)) \, u_{ji}(t) - v_{ij}(t) \, G_i(n_i(t)) \, (1 - u_{ij}(t)) \Big\}$$

where $q_i(t) = q_{ii}(t) + q_{ij}(t)$, $i, j = 1, 2$. $G_i(n_i(t))$ is the trip completion flow of Region i at time t, $v_{ji}(t) G_j(n_j(t)) u_j(t)$ is the cross-boundary trip completion flow from Region j to Region i, and $v_{ij}(t) G_i(n_i(t)) \cdot (1 - u_i(t))$ is the remaining transfer flow from Region j to Region i.

(iv) For a multi-region MFD system with control, i.e., (1a)-(1b), the **admissible travel demand** $\tilde{q}_i(t)$ with given control for Region i can be defined as

$$\tilde{q}_i(t) = \min\Big\{ q_i(t), G_i(n_i) - \sum_{j \in S_i} v_{ij} G_i(n_i) \cdot (1 - u_{ij}) - \sum_{j \in S_i} v_{ji} G_j(n_j) \cdot u_{ji} \Big\}$$

where $q_i(t) = q_{ii}(t) + \sum_{j \in S_i} q_{ij}(t)$, $i = 1, \ldots, L$, $j \in S_i$. $G_i(n_i(t))$ is the trip completion flow of Region i at time t, $\sum_{j \in S_i} v_{ji} G_j(n_j) \cdot u_{ji}$ is the cross-boundary trip completion flow heading to Region i, and $\sum_{j \in S_i} v_{ij} G_i(n_i) \cdot (1 - u_{ij})$ is the remaining transfer flow intending to leave Region i. In particular, $q_i(t) \equiv \bar{q}_i = \bar{q}_{ii} + \sum_{j \in S_i} \bar{q}_{ij}$ for the constant demand case. ∎

4.2. Stability analysis for single-region MFD system without control

Definition 4.2. For the single-region MFD system with constant demand but no control, i.e., (5), the **strictly admissible** travel demand $\tilde{q}(t)$ can be thus defined:

$$\tilde{q}(t) = \begin{cases} \min\{\bar{q}, G^{\max}\}, & 0 < n(t) \le \bar{n}^s \\ \min\{\bar{q}, G(n(t))\}, & \bar{n}^s < n(t) < \bar{n}^u \\ \min\{\bar{q}, G(n(t)) - \epsilon\}, & \bar{n}^u \le n(t) < n_{jam} \end{cases} \tag{10}$$

where $\epsilon \in \mathbb{R}_+$ is an arbitrary small number. ∎

Remark 4.1. Gayah and Daganzo (2011) found that the MFD becomes more scattered at a high accumulation state and that the network tends to become jammed at lower accumulation state than the theoretical one of the system. Such a point on the declining part of the MFD is known as the maximum sustainable accumulation. An exit function $G(n)$ that exceeds this value would result in a zero network trip completion flow, even though there are still vehicles remaining in the network (i.e., the network is trapped in gridlock under heavily congested conditions Daganzo, 2007; Mahmassani et al., 2013). To avoid this, we impose a constant $\epsilon > 0$ to guarantee the strict feasibility of Equation (10) for mathematical completeness, to keep the MFD well-defined from theoretical consideration and to protect the network from gridlock from practical consideration. ∎

Under Definition 4.2, system (5) admits a unique equilibrium. To see this, when $n = \bar{n}^u$, we have

$$\tilde{q} = \min\{\bar{q}, G(n(t)) - \epsilon\} < G(n(t)) \quad \Rightarrow \quad \dot{n} = \tilde{q} - G(n(t)) \le G(n(t)) - \epsilon - G(n(t)) = -\epsilon < 0$$

Therefore, there only exists one equilibrium $\bar{n}^s$ such that $\dot{n} = \tilde{q} - G(n(t)) = 0$.

Parallel to Gomes et al. (2008), wherein the stability of the CTM was analyzed under strictly feasible constant travel demand, we analyze in this subsection the stability of the equilibria induced by a feasible constant travel demand per Theorem 3.1 for the single-region MFD system without control (5) under admissible travel demand per (9) of Definition 4.1 and under strictly admissible travel demand per Definition 4.2, respectively.

Lemma 4.1. For equilibria $\bar{n}_s$ and $\bar{n}_u$ of (5) induced by a feasible constant travel demand per Theorem 3.1, we have:

(i) With **admissible** travel demand per (9) of Definition 4.1, the equilibrium $\bar{n}^s$ is locally stable on $[0, \bar{n}^u)$, which indicates that the trajectory that starts from the left side of the unstable equilibrium $\bar{n}^u$ converges to the uncongested equilibrium $\bar{n}^s$. Otherwise, the trajectory that starts from the right side of the unstable equilibrium $\bar{n}^u$ remains in its initial state.

$$\lim_{\substack{t \to \infty \\ 0 \le n(0) < \bar{n}^u}} n(t) = \bar{n}^s, \quad \lim_{\substack{t \to \infty \\ \bar{n}^u \le n(0) < n_{jam}}} n(t) = n(0)$$

(ii) With **strictly admissible** travel demand per Definition 4.2, the equilibrium $\bar{n}^s$ is globally stable on $[0, n_{jam})$, i.e., the state trajectory will converge to the stable uncongested equilibrium $\bar{n}^s$.

$$\lim_{\substack{t \to \infty \\ 0 \le n(0) < n_{jam}}} n(t) = \bar{n}^s$$

∎

PROOF OF LEMMA 4.1. Refer to Appendix C. ∎

Remark 4.2. The steady state of travel demand is essential in the MFD framework. It is believed that if demand evolves slowly over time, the steady state of the system can be achieved. Given the steady state of travel demand, the equilibria of the system can be determined by solving the steady-state equations. However, the concept of a steady state of a road network has not been clearly defined in the MFD literature (Jin et al., 2013). No uniform definition of the steady state of travel demand is recognized in the MFD literature. This renders identification of a steady state from a time-varying demand profile (especially for the fast time-varying case) a significantly difficult and unclear task in practice. ∎

4.3. Admissible travel demand and controllability

To handle the above mentioned hurdles caused by time-varying travel demand, we extend the proposed admissible travel demand concept to investigate the controllability of the MFD system under time-varying demand. Given the desired traffic equilibrium, for a single-region MFD system, Haddad and Shraiber (2014) derived a sufficient condition for controllability with respect to travel demand during the transient period, that is, the time period in which the initial state is brought to the steady state. To increase or decrease the state to the steady-state state, the conditions $dn_i/dt > 0$ or $dn_i/dt < 0$ should be satisfied, respectively. We extend this result for our three cases in this subsection.

Proposition 4.1. Given the target uncongested equilibrium $\bar{n}_i^s$ of the multi-region MFD system described by (2), if the travel demand $q_i(t)$ satisfies

$$q_i(t) < G_i(n_i(t)) - \sum_{j \in S_i} v_{ij}(t) G_i(n_i(t)) (1 - u_{ij}(t)) - \sum_{j \in S_i} v_{ji}(t) G_j(n_j(t)) u_{ji}(t), \quad \text{if } n_i(t) > \bar{n}_i^s \quad \text{(11a)}$$

$$q_i(t) > G_i(n_i(t)) - \sum_{j \in S_i} v_{ij}(t) G_i(n_i(t)) (1 - u_{ij}(t)) - \sum_{j \in S_i} v_{ji}(t) G_j(n_j(t)) u_{ji}(t), \quad \text{if } n_i(t) < \bar{n}_i^s \quad \text{(11b)}$$

13

for $i = 1, \ldots, L$, $j \in S_i$, during the transient period, then the MFD system is controllable. ∎

PROOF OF PROPOSITION 4.1. If $n_i(t) > \bar{n}_i^s$, the condition $\frac{\mathrm{d}n_i}{\mathrm{d}t} < 0$ should be satisfied to decrease the state to the steady-state point. Because

$$\frac{\mathrm{d}n_i}{\mathrm{d}t} = -\Big[G_i(n_i) - \sum_{j \in S_i} v_{ij} G_i(n_i) \cdot (1 - u_{ij}) - \sum_{j \in S_i} v_{ji} G_j(n_j) \cdot u_{ji} \Big] + q_i(t) < 0.$$

This implies the condition (11a).

Otherwise if $n_i(t) < \bar{n}_i^s$, the condition $\frac{\mathrm{d}n_i}{\mathrm{d}t} > 0$ should be satisfied to increase the state to the steady-state point. Because

$$\frac{\mathrm{d}n_i}{\mathrm{d}t} = -\Big[G_i(n_i) - \sum_{j \in S_i} v_{ij} G_i(n_i) \cdot (1 - u_{ij}) - \sum_{j \in S_i} v_{ji} G_j(n_j) \cdot u_{ji} \Big] + q_i(t) > 0.$$

This implies the condition (11b). ∎

Proposition 4.2. Given the target uncongested equilibrium $\bar{n}_1^s$ of the single-region MFD system with perimeter control (4), if the travel demand $q(t)$ satisfies

$$q(t) < G_1(n_1(t)) - \big(q_{21}(t) + (1 - v(t)) G_1(n_1(t)) \big) \big(1 - u(t) \big), \quad \text{if } n_1(t) > \bar{n}_1^s \tag{12a}$$

$$q(t) > G_1(n_1(t)) - \big(q_{21}(t) + (1 - v(t)) G_1(n_1(t)) \big) \big(1 - u(t) \big), \quad \text{if } n_1(t) < \bar{n}_1^s \tag{12b}$$

during the transient period, then the MFD system is controllable. ∎

PROOF OF PROPOSITION 4.2. If $n_1(t) > \bar{n}_1^s$, the condition $\frac{\mathrm{d}n_1}{\mathrm{d}t} < 0$ should be satisfied to decrease the state to the steady state. Because

$$\frac{\mathrm{d}n_1}{\mathrm{d}t} = q(t) - \Big[G_1(n_1(t)) - \big(q_{21}(t) + (1 - v(t)) G_1(n_1(t)) \big) \big(1 - u(t) \big) \Big] < 0$$

This implies the condition (12a).

If instead $n_1(t) < \bar{n}_1^s$, the condition $\frac{\mathrm{d}n_1}{\mathrm{d}t} > 0$ should be satisfied to increase the state to the steady state. Because

$$\frac{\mathrm{d}n_1}{\mathrm{d}t} = q(t) - \Big[G_1(n_1(t)) - \big(q_{21}(t) + (1 - v(t)) G_1(n_1(t)) \big) \big(1 - u(t) \big) \Big] > 0$$

This implies the condition (12b). ∎

Proposition 4.3. Given the target uncongested equilibrium $\bar{n}^s = [\bar{n}_1^s, \bar{n}_2^s]^T$ of the two-state two-region MFD system described by (8a)-(8b), if the travel demand $q(t) = [q_1(t), q_2(t)]^T$ satisfies

$$q_i(t) < G_i(n_i(t)) - v_{ji}(t) G_j(n_j(t)) u_{ji}(t) - v_{ij}(t) G_i(n_i(t)) (1 - u_{ij}(t)), \quad \text{if } n_i(t) > \bar{n}_i^s \tag{13a}$$

$$q_i(t) > G_i(n_i(t)) - v_{ji}(t) G_j(n_j(t)) u_{ji}(t) - v_{ij}(t) G_i(n_i(t)) (1 - u_{ij}(t)), \quad \text{if } n_i(t) < \bar{n}_i^s \tag{13b}$$

for $i, j = 1, 2$, during the transient period, then the MFD system is controllable. ∎

Proof of Proposition 4.3. The proof of Proposition 4.3 can be deduced from the proof of Proposition 4.1 by $L = 2$. ∎

As previously discussed, two equilibria, $\bar{n}^s$ and $\bar{n}^u$, can be identified by solving the steady-state equations (see for example Figure 3). Under the admissible travel demand, $\bar{n}^s$ is locally stable on $[0, \bar{n}^u)$ whilst $\bar{n}^u$ is unstable (see for example Lemma 4.1). Therefore, $\bar{n}^s$ is more likely to be a desired equilibrium for control design. On the other hand, as discussed in Remark 4.2, the steady state of a time-varying travel demand is not well-defined in the MFD literature. Although the traffic manager may have difficulties in calibrating a functional form and its steady state for the time-varying demand, he or she definitely has a preferable network condition (or state) for management purposes. He or she can infer a stationary demand from the target network state and define it as a desired steady state for the time-varying demand, that is, a 'priori'. To enable the traffic manager to enforce his or her 'priori' regardless of the true steady state (that is a 'miracle' to him or her) such that the management objective, that is, $\bar{n}^s$, is attainable, we refine the admissible travel demand with strictly admissible travel demand that satisfies the sufficient conditions in Proposition 4.1-Proposition 4.3 and thus guarantees the systems' controllability.

Definition 4.3. (**strictly admissible travel demand**) (i) For the single-region MFD system with control and feasible demand, i.e., (4), the **strictly admissible** travel demand $\tilde{q}(t)$ with given perimeter control can be thus defined:

$$
\tilde{q}(t) = \begin{cases}
\text{mid}\Big\{q(t), G_1(n_1(t)) - \big(q_{21}(t) + (1-\upsilon(t))G_1(n_1(t))\big)(1-u(t)) + \epsilon_1, G_1(n_1(t))\Big\}, & 0 < n_1(t) < \bar{n}_1^s \\
\min\Big\{q(t), G_1(n_1(t)) - \big(q_{21}(t) + (1-\upsilon(t))G_1(n_1(t))\big)(1-u(t))\Big\}, & \bar{n}_1^s \le n_1(t) < \bar{n}_1^u \\
\min\Big\{q(t), G_1(n_1(t)) - \big(q_{21}(t) + (1-\upsilon(t))G_1(n_1(t))\big)(1-u(t)) - \epsilon_2\Big\}, & \bar{n}_1^u \le n_1(t) < n_{1,jam}
\end{cases}
\tag{14}
$$

where ϵ_i with $i = 1, 2$ is an arbitrary small number, and 'mid' denotes the middle of the three points. In particular, $q(t) \equiv \bar{q}$ for the constant demand case.

(ii) Given the two-region MFD system (8a)-(8b) with feasible demand, the **strictly admissible** travel demand $\tilde{q}_i(t)$ with given perimeter control for Region i, where $i = 1, 2$, is

$$
\tilde{q}_i(t) = \begin{cases}
\text{mid}\Big\{q_i(t), G_i(n_i(t)) - \upsilon_{ji}(t)G_j(n_j(t))u_{ji}(t) - \upsilon_{ij}(t)G_i(n_i(t))(1-u_{ij}(t)) + \epsilon_i, G_i(n_i(t))\Big\}, & 0 < n_i(t) < \bar{n}_i^s \\
\min\Big\{q_i(t), G_i(n_i(t)) - \upsilon_{ji}(t)G_j(n_j(t))u_{ji}(t) - \upsilon_{ij}(t)G_i(n_i(t))(1-u_{ij}(t))\Big\}, & \bar{n}_i^s \le n_i(t) < \bar{n}_i^u \\
\min\Big\{q_i(t), G_i(n_i(t)) - \upsilon_{ji}(t)G_j(n_j(t))u_{ji}(t) - \upsilon_{ij}(t)G_i(n_i(t))(1-u_{ij}(t)) - \epsilon_i\Big\}, & \bar{n}_i^u \le n_i(t) < n_{i,jam}
\end{cases}
\tag{15}
$$

where $\epsilon_i \in \mathbb{R}_+$ is an arbitrary small number. In particular, $q_i(t) \equiv \bar{q}_i$ for the constant demand case.

(iii) Given the multi-region MFD system (2) with feasible demand, the **strictly admissible** travel demand $\tilde{q}_i(t)$ with given perimeter control for Region i, where $i = 1, \ldots, L, \ j \in S_i$, is

$$
\tilde{q}_i(t) = \begin{cases}
\text{mid}\Big\{q_i(t), G_i(n_i(t)) - \sum_{j \in S_i}\upsilon_{ij}(t)G_i(n_i(t))(1-u_{ij}(t)) - \sum_{j \in S_i}\upsilon_{ji}(t)G_j(n_j(t))u_{ji}(t) + \epsilon_i, G_i(n_i(t))\Big\}, & 0 < n_i(t) < \bar{n}_i^s \\
\min\Big\{q_i(t), G_i(n_i(t)) - \sum_{j \in S_i}\upsilon_{ij}(t)G_i(n_i(t))(1-u_{ij}(t)) - \sum_{j \in S_i}\upsilon_{ji}(t)G_j(n_j(t))u_{ji}(t)\Big\}, & \bar{n}_i^s \le n_i(t) < \bar{n}_i^u \\
\min\Big\{q_i(t), G_i(n_i(t)) - \sum_{j \in S_i}\upsilon_{ij}(t)G_i(n_i(t))(1-u_{ij}(t)) - \sum_{j \in S_i}\upsilon_{ji}(t)G_j(n_j(t))u_{ji}(t) - \epsilon_i\Big\}, & \bar{n}_i^u \le n_i(t) < n_{i,jam}
\end{cases}
\tag{16}
$$

where $\epsilon_i \in \mathbb{R}_+$ is an arbitrary small number. In particular, $q_i(t) \equiv \bar{q}_i$ for the constant demand case. ∎

The 'mid' operator is defined in light of the merge and diverge representations depicted in Daganzo (1995). To see this, as shown in Figure 2(b), the flows merging into Region 1 are $\upsilon_{21}(t)G_2(n_2(t))u_{21}(t)$, the

transferring flow from Region 2 to Region 1, and $q_1(t)$, the demand of Region 1. Flows $v_{12}(t)G_1(n_1(t))u_{12}(t)$ from Region 1 to Region 2, and $v_{11}(t)G_1(n_1(t))$, the trip completed into sink 1, diverge from Region 1. In line with Daganzo (1995), the solution for the merge operation is the middle of the three points, that is, the current demand, the available space and the ideal trip completion flow. Thus, we write

$$\tilde{q}_1(t) = \text{mid}\Big\{ q_1(t), G_1(n_1(t)) - v_{21}(t)G_2(n_2(t))u_{21}(t) - v_{12}(t)G_1(n_1(t))(1 - u_{12}(t)) + \epsilon_1, G_1(n_1(t)) \Big\}, 0 < n_1(t) < \bar{n}_1^s$$

Regarding Figure 4, because the cross-boundary traffic is regulated by the perimeter (or gating) control, the amount of traffic determined by the perimeter control scheme should be received by the destination region, that is, Region 1. Therefore, the boundary condition should be imposed on the amount of traffic whose origin is Region 1 (i.e., q_1).
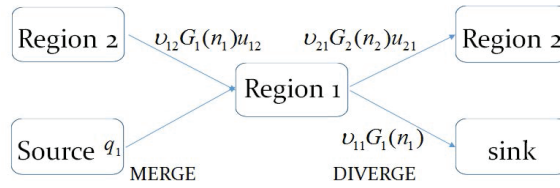

Figure 4: Analogue representation of a merge and diverge

Remark 4.3. The first equation of (15) implies (13a) while it is saturated by the throughput of the network $G_i(n_i)$. The second and third equations state that the inflow to the network should be the minimum of the demand and the available space. The constant $\epsilon > 0$ is used to guarantee the strict feasibility of (13a) and (13b) . The reason for the introduction of $\epsilon > 0$ in the third equation of (15) has been outlined in Remark 4.1. In this remark, we elaborate upon the plausibility of introducing $\epsilon > 0$ into the first equation of (15). Similar logic can be applied to (14) and (16).

Note that in the first equation of the above definition, when $n_i(t) < \bar{n}_i^s$, the *strictly admissible* travel demand loaded into the network would be $G_i(n_i(t)) - v_{ji}(t)G_j(n_j(t))u_{ji}(t)v_{ij}(t)G_i(n_i(t))(1 - u_{ij}(t)) + \epsilon_i$ if $q_i < G_i(n_i(t)) - v_{ji}(t)G_j(n_j(t))u_{ji}(t) - v_{ij}(t)G_i(n_i(t))(1 - u_{ij}(t)) + \epsilon_i$. That is, the actual demand is too small to allow the system to reach the desired equilibrium, so the 'demand' equal to the available space, rather than the actual demand, is loaded into the network. Intuitively, this has no physical meaning. For instance, when the demand is constant, loading a value larger than the demand is meaningless. On the other hand, this requirement stemmed from the unreasonable choice of the desired equilibrium $\bar{n}_i^s$, that is, setting $\bar{n}_i^s$ larger than the steady state that the demand pattern would yield. This is unnecessary and without practical consideration because the control objective is to make the network denser than it should be without any control. It is a waste of network capacity and control effort whilst causing larger network delays. For such a case, an easy and wise way is to choose a desired equilibrium less than (or be equal to) the steady state that the demand pattern would yield such that the demand is sufficiently large to fill the network and control effort is necessary. We demonstrate this again in the numerical examples. Here, we impose this simply to help maintain the mathematical completeness rather than for practical consideration. ∎

Controllability describes the ability of an external input to move the internal state of a dynamic system from an arbitrarily initial state to any other final state within a finite time interval. Note that controllability does not mean that a state can be maintained once it is reached, whilst stabilizability implies that the system under control is stable and that the desired state can thus be maintained. The objective of traffic control schemes is to move the traffic state from any initial condition to the desired equilibrium and to

16

maintain the desired state after it is reached. Therefore, in what follows, we investigate stabilizability rather than controllability. In the literature, Haddad and Mirkin (2016) developed feedback control schemes for single-region MFD system based on the model linearization using adaptive model reference control. Geroliminis et al. (2013) proposed optimal perimeter control for two-region MFD system using model predictive control without stability analysis. Zhong et al. (2017) investigated the robust stabilization of two-region MFD system against both noisy MFD and uncertain travel demand. Through the lens of control-Lyapunov function (CLF), closed-form feedback control schemes that determine the control in an automatic manner without adjusting extensive design parameters are obtained. Both global asymptotic stability and appealing robustness for the closed-loop MFD system are achieved.

Since the the equilibrium is not 0, we incorporate a coordinate transformation $\tilde{n} = n(t) - \bar{n}$ and $\tilde{u} = u(t) - \bar{u}$ such that 0 is the new equilibrium (refer to Appendix E for the two-region example). It follows from **Lyapunov's Theorem** and **Converse Lyapunov's Theorem** (see Haddad and Chellaboina, 2008, chap. 3) that the nonlinear dynamic system of the form (4) or (8a)-(8b) or (2) is feedback asymptotically stabilizable if and only if there exists a control-Lyapunov function thus defined:

Definition 4.4. (**Control-Lyapunov function**, see Haddad and Chellaboina, 2008, pg. 438) Consider the nonlinear dynamical system given by (4) or (8a)-(8b) or (2) with control input constraints $\tilde{u} \in \mathcal{K}$. A continuously differentiable positive-definite function $V : \mathcal{D} \to \mathbb{R}_+$ satisfying

$$\inf_{u \in \mathcal{K}} V'(\tilde{n})\dot{\tilde{n}} < 0, \quad \tilde{n} \in \mathcal{D}, \quad \tilde{n} \neq 0 \tag{17}$$

is called a **control-Lyapunov function**. Moreover, in the case where $\mathcal{D} = \mathbb{R}^L$, the zero solution $\tilde{n} \equiv 0$ to (4) or (8a)-(8b) or (2) is globally asymptotically stabilizable, respectively, if and only if $V(\tilde{n})$ is *radially unbounded*, i.e., $V(\tilde{n}) \to \infty$ as $\|\tilde{n}\| \to \infty$. ∎

According to the characteristics of the MFD systems, three quadratic functions of $\tilde{n}$, $V(\tilde{n}_1) = \frac{1}{2}\tilde{n}_1^2$, $V(\tilde{n}) = \frac{1}{2}\tilde{n}_1^2 + \frac{1}{2}\tilde{n}_2^2$, and $V(\tilde{n}) = \frac{1}{2}\sum_{i=1}^{L}\tilde{n}_i^2$ could be the CLF candidates for single-region, two-region and multi-region MFD systems, respectively. The following theorem and its corollaries verify this hypothesis.

Theorem 4.1. The function $V(\tilde{n}) = \frac{1}{2}\sum_{i=1}^{L}\tilde{n}_i^2$ is a CLF for the multi-region MFD system (2) with strictly admissible travel demand per (16). Therefore, the equilibrium $\bar{n}_i^s$ of the closed-loop system composed of (2) with strictly admissible travel demand per (16) can be made globally asymptotically stable by suitable control whose steady state is $\bar{u}_{ij}$, $i = 1, \ldots, L$, $j \in S_i$. ∎

PROOF OF THEOREM 4.1. It is trivial to prove that $V(\tilde{n})$ is positive-definite, continuously differentiable and radially unbounded. Therefore what remains is to verify (17) holds. Note that $V'(\tilde{n}) = [\tilde{n}_1, \ldots, \tilde{n}_L]$, one obtains

$$\begin{aligned}\inf_{\tilde{u} \in \mathcal{K}} \dot{V}(t) &= \sum_{i=1}^{L}\tilde{n}_i \cdot \dot{\tilde{n}}_i = \sum_{i=1}^{L}\tilde{n}_i \cdot \dot{n}_i \\ &= \sum_{i=1}^{L}\tilde{n}_i\left\{q_i - \left[G_i(n_i) - \sum_{j \in S_i}\upsilon_{ij}G_i(n_i) \cdot (1 - u_{ij}) - \sum_{j \in S_i}\upsilon_{ji}G_j(n_j) \cdot u_{ji}\right]\right\}\end{aligned} \tag{18}$$

For the special case when $\tilde{q}_i \equiv 0$, i.e., zero travel demand, traffic state is excited by the initial condition which will evolve to the origin $[0, \ldots, 0]^T$ eventually. Then $\tilde{n} = n \in \mathbb{R}_+^L$. There exists a control input u_{ij}, $i = 1, \ldots, L$, $j \in S_i$ such that for $i = 1, \ldots, L$,

$$\frac{dn_i}{dt} = -G_i(n_i) + \sum_{j \in S_i}\upsilon_{ij}G_i(n_i) \cdot (1 - u_{ij}) - \sum_{j \in S_i}\upsilon_{ji}G_j(n_j) \cdot u_{ji} < 0$$

17

By simply choosing $u_{ij} = 0$, $i = 1, \ldots, L$, $j \in S_i$, by noting that when the demand pattern is zero there is no cross boundary flow, then one gets

$$\dot{V}(t) = \sum_{i=1}^{L} \tilde{n}_i \cdot \dot{n}_i = -\sum_{i=1}^{L} n_i \cdot G_i(n_i) < 0, \ \ \text{if} \ \ n \neq 0$$

Since the origin is the only point contained by the largest invariant set in $\mathcal{R} \triangleq \left\{ n(t) \in \mathcal{N} : \dot{V}(n) = 0 \right\}$, by LaSalle's invariance theorem, we have $n(t) \to 0$ as $t \to \infty$. When instead $\tilde{q}_i \not\equiv 0$, the following discussion is divided into threefold:

First, if $0 < n_i < \bar{n}_i^s$, one gets $\tilde{n}_i = n_i - \bar{n}_i^s < 0$.

(i) Suppose $q_i \le G_i(n_i) - \sum_{j \in S_i} v_{ij} G_i(n_i) \cdot (1 - u_{ij}) - \sum_{j \in S_i} v_{ji} G_j(n_j) \cdot u_{ji} + \epsilon_i \le G_i(n_i)$, then from (16), we have

$$\tilde{q}_i = G_i(n_i) - \sum_{j \in S_i} v_{ij} G_i(n_i) \cdot (1 - u_{ij}) - \sum_{j \in S_i} v_{ji} G_j(n_j) \cdot u_{ji} + \epsilon_i.$$

Then

$$\frac{d\tilde{n}_i}{dt} = -G_i(n_i) + \sum_{j \in S_i} v_{ij} G_i(n_i) \cdot (1 - u_{ij}) + \sum_{j \in S_i} v_{ji} G_j(n_j) \cdot u_{ji} + \tilde{q}_i = \epsilon_i > 0,$$

so that $\tilde{n}_i \cdot \frac{d\tilde{n}_i}{dt} < 0$;

(ii) Suppose $G_i(n_i) - \sum_{j \in S_i} v_{ij} G_i(n_i) \cdot (1 - u_{ij}) - \sum_{j \in S_i} v_{ji} G_j(n_j) \cdot u_{ji} + \epsilon_i \le q_i \le G_i(n_i)$, one obtains $\tilde{q}_i = q_i$. Then

$$\frac{d\tilde{n}_i}{dt} = -G_i(n_i) + \sum_{j \in S_i} v_{ij} G_i(n_i) \cdot (1 - u_{ij}) + \sum_{j \in S_i} v_{ji} G_j(n_j) \cdot u_{ji} + q_i \ge \epsilon_i > 0,$$

so that $\tilde{n}_i \cdot \frac{d\tilde{n}_i}{dt} < 0$;

(iii) Suppose $G_i(n_i) - \sum_{j \in S_i} v_{ij} G_i(n_i) \cdot (1 - u_{ij}) - \sum_{j \in S_i} v_{ji} G_j(n_j) \cdot u_{ji} + \epsilon_i \le G_i(n_i) \le q_i$, one obtains $\tilde{q}_i = G_i(n_i)$.

Then

$$\frac{d\tilde{n}_i}{dt} = -G_i(n_i) + \sum_{j \in S_i} v_{ij} G_i(n_i) \cdot (1 - u_{ij}) + \sum_{j \in S_i} v_{ji} G_j(n_j) \cdot u_{ji} + G_i(n_i) = \sum_{j \in S_i} v_{ij} G_i(n_i) \cdot (1 - u_{ij}) + \sum_{j \in S_i} v_{ji} G_j(n_j) \cdot u_{ji} > 0,$$

so that $\tilde{n}_i \cdot \frac{d\tilde{n}_i}{dt} < 0$. Thus, for this case, we have $\dot{V}(t) < 0$.

Second, if $\bar{n}_i^s \le n_i < \bar{n}_i^u$, one gets $\tilde{n}_i = n_i - \bar{n}_i^s \ge 0$, from (16) we have

$$
\begin{aligned}
\tilde{q}_i \ & \le \ G_i(n_i) - \sum_{j \in S_i} v_{ij} G_i(n_i) \cdot (1 - u_{ij}) - \sum_{j \in S_i} v_{ji} G_j(n_j) \cdot u_{ji} \\
& = \ -\left[-G_i(n_i) + \sum_{j \in S_i} v_{ij} G_i(n_i) \cdot (1 - u_{ij}) + \sum_{j \in S_i} v_{ji} G_j(n_j) \cdot u_{ji} \right]
\end{aligned}
$$

then

$$\frac{d\tilde{n}_i}{dt} = -\left[G_i(n_i) - \sum_{j \in S_i} v_{ij} G_i(n_i) \cdot (1 - u_{ij}) - \sum_{j \in S_i} v_{ji} G_j(n_j) \cdot u_{ji} \right] + \tilde{q}_i \le 0,$$

so that $\tilde{n}_i \cdot \frac{d\tilde{n}_i}{dt} \le 0$. Now, we need to show $\dot{V}(t) = 0$ if and only if $n_i = \bar{n}_i^s$. If $\frac{d\tilde{n}_i}{dt} = 0$, we have the system satisfies the steady-state equations (A.13a)-(A.13b). This implies $n = \bar{n}_i^s$ as $n = \bar{n}_i^u$ is excluded in this interval.

18

Finally, if $\bar{n}_i^u \le n_i < n_i^{jam}$, one gets $\tilde{n}_i = n_i - \bar{n}_i^s > 0$, from (16) we have

$$
\begin{aligned}
\tilde{q}_i &\le G_i(n_i) - \sum_{j \in S_i} \upsilon_{ij} G_i(n_i) \cdot (1 - u_{ij}) - \sum_{j \in S_i} \upsilon_{ji} G_j(n_j) \cdot u_{ji} - \epsilon_i \\
&= -\left[-G_i(n_i) + \sum_{j \in S_i} \upsilon_{ij} G_i(n_i) \cdot (1 - u_{ij}) + \sum_{j \in S_i} \upsilon_{ji} G_j(n_j) \cdot u_{ji} + \epsilon_i \right]
\end{aligned}
$$

then

$$
\frac{\mathrm{d}\tilde{n}_i}{\mathrm{d}t} = -G_i(n_i) + \sum_{j \in S_i} \upsilon_{ij} G_i(n_i) \cdot (1 - u_{ij}) + \sum_{j \in S_i} \upsilon_{ji} G_j(n_j) \cdot u_{ji} + \tilde{q}_i \le -\epsilon_i < 0
$$

so that $\tilde{n}_i \cdot \frac{\mathrm{d}\tilde{n}_i}{\mathrm{d}t} < 0$.

To close the discussion, it follows that for $i = 1, \ldots, L$, $\tilde{n}_i$ and $\frac{\mathrm{d}n_i}{\mathrm{d}t}$ have opposite signs while $\tilde{n}_i \ne 0$, i.e. , $\tilde{n}_i < 0 \; (> 0)$ as long as $\frac{\mathrm{d}n_i}{\mathrm{d}t} > 0 \; (< 0)$. Then while $\tilde{n}_i \ne 0$ we always have $\tilde{n}_i \cdot \frac{\mathrm{d}n_i}{\mathrm{d}t} < 0$. Therefore, $V'(\tilde{n})\dot{n} < 0$ when $\tilde{n} \ne 0$.

On the other hand, $V'(\tilde{n}) = [0, \ldots, 0]$ while $\tilde{n}_i = 0$. So obviously $V'(\tilde{n})\dot{n} = 0$ if $\tilde{n}_i = 0$, then one gets

$$
V'(\tilde{n})\dot{n} = \begin{cases} \tilde{n}_i \cdot \frac{\mathrm{d}n_i}{\mathrm{d}t} < 0, & \tilde{n} \ne 0, \\ 0, & \tilde{n} = 0. \end{cases} \tag{19}
$$

Thus from Definition 4.4, the function $V(\tilde{n}) = \frac{1}{2} \sum_{i=1}^{L} \tilde{n}_i^2$, satisfying (17), is a CLF for system (2), which guarantees the system's global stabilizability. ∎

Corollary 4.1. The function $V(\tilde{n}) = \frac{1}{2}\tilde{n}_1^2 + \frac{1}{2}\tilde{n}_2^2$ is a CLF for system (8a)-(8b) with strictly admissible travel demand per (15). The desired equilibrium $\bar{n}^s = [\bar{n}_1^s, \bar{n}_2^s]^T$ of the closed-loop system composed of (8a)-(8b) with strictly admissible travel demand per (15) can be made globally asymptotically stable by suitable control whose steady state is $\bar{u} = [\bar{u}_{12}, \bar{u}_{21}]^T$. ∎

PROOF OF COROLLARY 4.1. The proof of Corollary 4.1 can be deduced from the proof of Theorem 4.1 by $L = 2$. Interested readers may also refer to Zhong et al. (2017) for the details of the proof. ∎

Corollary 4.2. The function $V(\tilde{n}_1) = \frac{1}{2}\tilde{n}_1^2$ is a CLF for system (4) with strictly admissible travel demand per (14). Therefore, the closed-loop system composed of (4) with strictly admissible travel demand per (14) can be stabilized by suitable control whose steady state is $\bar{u}$. ∎

PROOF OF COROLLARY 4.2. The proof of this corollary can be deduced from that of Theorem 4.1. A detailed proof is presented in Appendix D. ∎

Remark 4.4. A direct implication by Theorem 4.1 and its corollaries is that any perimeter control, that can regulate the traffic state to the target equilibrium, has to converge to the corresponding steady state obtained from the steady-state equations. If there is no other effective method or the traffic manager is just lazy, the perimeter control gain can be simply chosen as its desired steady state. ∎

4.4. Discussion and implications

Conventionally, market-based approaches, such as road pricing (Zheng et al., 2012, 2016), and traffic flow control approaches, such as perimeter control, are frequently applied to regulate traffic flow in urban transportation networks to improve their efficiency. To avoid political resistance to congestion charges, some researchers and planners have turned to quantity control to restrict the use of private vehicles. To be specific, in a quantity control scheme, the authority determines the travel demand to be served and then assigns fixed mobility rights equally to all individual travelers or inhabitants so that fairness is explicitly demonstrated (Yang and Wang, 2011). The simplest quantity control method is the plate-number-based traffic rationing, such as the temporary plate-number-based traffic rationing in Beijing and Guangzhou in China and some long-term applications of road space rationing in Latin America, such as those in Mexico City, Santiago and São Paulo. In the literature, these categories of traffic management schemes are developed independently. However, in practice, a traffic network would have all of these traffic management schemes simultaneously, or at least a hybrid of them, such as road pricing and traffic flow controls. It would be interesting to examine the performance of hybrid combinations of these traffic management schemes (Zhong et al., 2014). The above developments assumed that the network is managed by a central authority with the objective of enhancing the performance of the entire network, which forms a closed system with boundaries. In practice, however, a transportation network would seldom form a closed system due to the inherent cross-boundary traffic. On a federal/state level, there are multiple administrative regions with each local region authority managing its local transportation subnetwork. When designing a transportation policy, a local transportation authority would maximize the social welfare of its residents only. For example, cities such as Hong Kong and Macao, with well-defined geographical limits due to their special administration, may maximize the social welfare of their local residents only. However, due to certain necessary daily activities, such as politics, tourism and logistics, there is cross-boundary traffic into and out of the local traffic network. A traffic manager needs to reserve a certain level of network capacity for cross-boundary traffic. For single-region and two-region MFD systems, each administrative region with local authority manages its local transportation subnetwork and always seeks to maximize the social welfare of its residents in the presence of cross boundary traffic. Therefore, given the cross boundary travel demand, the authority administrator or traffic manager would determine the desired steady-state transfer rate of the cross-boundary traffic according to the travel demand from the steady-state equations.

Corollary 4.2, Corollary 4.1 and Theorem 4.1 imply that network traffic can converge to the desired uncongested equilibrium by means of any perimeter control scheme whose steady state equals the desired steady state of the cross-boundary traffic. This surprising finding indicates that the perimeter control can be simply chosen as its desired steady state, that is, $\bar{u}$ such that the network traffic dynamics governed by (4), (8a)-(8b) and (2) can be regulated to the desired uncongested equilibrium $\bar{n}^s$, under the strictly admissible travel demand per (14), per (15) and per (16), respectively. Parallel to the perimeter control, market-based traffic control schemes, such as road pricing to charge the cross-boundary traffic for accessing the local network, can be also developed. For example, an off-line dynamic pricing scheme can be devised based on the calibrated MFD system and the demand pattern from the observed historical traffic dynamics. In the literature, dynamic toll schemes are devised based on the difference between the delay cost during the transient periods and steady-state delay cost (Zheng et al., 2012, 2016; Simoni et al., 2015). Zheng et al. (2012, 2016) proposed a proportional or proportional-integral (PI) type controller of the following form

$$Toll_{i+1}(t) = Toll_i(t) + c_1(K_i(t) - \bar{K}) + c_2(K_i(t) - K_{i-1}(t)) \tag{20}$$

to regulate the network state $K(t)$ (in terms of density) to a desired state $\bar{K}$ by choosing appropriate values of parameters c_1 and c_2, where i is the i-th adjustment of the toll at time interval t and the desired state is

often specified as the critical network density K_{cr}. The toll at the $(i + 1)$-th toll adjustment for time interval t, $Toll_{i+1}(t)$, is proportional to the magnitude to which the average network density $K(t)$ exceeds $\bar{K}$ and the difference between the resultant densities under the current pricing $K_i(t)$ and the previous one $K_{i-1}(t)$. Zheng et al. (2016) commented that an analytical solution for c_1 and c_2 would be impossible to obtain because of the complex network dynamics. Therefore, the parameters c_1 and c_2 are chosen off-line via a trial-and-error process to avoid oscillations. With mapping that converts a traffic flow measure to a monetary measure through network delay and average value of time (VOT) similar to that of Zheng et al. (2012, 2016); Simoni et al. (2015), a tolling scheme can be developed similar to the perimeter control. To see this, let the perimeter control gain function be at its steady state (determined from the desired cross-boundary traffic flow), i.e., $\bar{u}$, for single-region MFD system (4),

$$\dot{\tilde{n}}_1 = -\left[\upsilon G_1(\tilde{n}_1 + \bar{n}_1) - \bar{\upsilon}G_1(\bar{n}_1)\right] - \left\{\left[q_{21} + (1 - \upsilon)G_1(\tilde{n}_1 + \bar{n}_1)\right] - \left[\bar{q}_{21} + (1 - \bar{\upsilon})G_1(\bar{n}_1)\right]\right\}\bar{u} + \tilde{q}_1 - \bar{q}_1 + q_{21} - \bar{q}_{21}$$

where $(1 - \upsilon)G_1(\tilde{n}_1 + \bar{n}_1)$ are the actual cross-boundary flows, whilst $(1 - \bar{\upsilon})G_1(\bar{n}_1)$ are the desired cross-boundary flows, respectively. The quantity $\left[(1 - \upsilon)G_1(\tilde{n}_1 + \bar{n}_1) - (1 - \bar{\upsilon})G_1(\bar{n}_1)\right]\bar{u}$ is a proportional feedback controller that stabilizes the system. Thus $\bar{u}$ can be regarded as an analytical solution for c_1 if only the proportional feedback control is adopted in (20) in line with Zheng et al. (2012). From the PID control theory, the integral part of the PI controller mainly governs the steady-state error (Ogata, 2010). If the proportional part can already stabilize the system (e.g., Corollary 4.2), we have a degree of freedom in choosing c_2 for the stabilization problem. For a demonstration purpose, a toll scheme is constructed as

$$\text{Toll} = c_1\left[(1 - \upsilon)G_1(\tilde{n}_1 + \bar{n}_1) - (1 - \bar{\upsilon})G_1(\bar{n}_1)\right], \quad c_1 = \text{VOT} \cdot \frac{\bar{n}_1}{G_1(\bar{n}_1)} \tag{21}$$

where $\frac{\bar{n}_1}{G_1(\bar{n}_1)}$ is the network average travel delay.

Whilst a constant perimeter control gain can guarantee the stability and convergence of the traffic dynamics to the desired equilibrium, as it will be shown later, a dynamic feedback controller (much more complex) can induce a much faster convergence rate and is thus more efficient. However, there is always a trade-off between the complexity and efficiency. On the other hand, a traffic rationing scheme can be implemented in line with the boundary conditions governed by the strictly admissible travel demand to protect the region from congestion.

5. Numerical simulations

In this section, we present simulation results to demonstrate the theoretical development. The functional form of the MFD is adopted from Geroliminis and Daganzo (2008); Haddad (2015), i.e.,

$$G_i(n_i) = \frac{1.4877 \cdot 10^{-7}n_i^3 - 2.9815 \cdot 10^{-3}n_i^2 + 15.0912n_i}{3600}, \; n_{i,cr} = 3400, \, G_i(n_{i,cr}) = 6.3, \, n_{i,jam} = 10000 \tag{22}$$

for single-region, two-region and three-region MFD systems. Furthermore, time-varying demand patterns, see Figure 5, are considered for one-region and two-region MFD systems.

5.1. Single-region MFD system without control

We first apply the proposed admissible travel demand and strictly admissible travel demand to the single-region MFD system. For a simple demonstration, the perimeter control is not considered in this example. For a comparison, both constant demand and time-varying demand are used. The constant demand under

consideration is $\bar{q} = 4$ (veh/s). Accordingly, this demand pattern induces two equilibria, i.e., $\bar{n}^s = 1238$ (veh) and $\bar{n}^u = 6202$ (veh), to the MFD system. Figure 6 depicts the state trajectories driven by this *constant demand* pattern with different initial accumulation states at $n(0) = 500, 3000, 5000, 8000$ (veh), respectively. From Figure 6(a), we can infer that under *admissible demand* constraint, the trajectories starting from the left side of $\bar{n}^u$, i.e., $n(0) = 500, 3000, 5000$ (veh), can converge to $\bar{n}^s$ as expected whilst that starting from the right side, $n(0) = 8000$ (veh), remains unchanged in its initial state. This is consistent with Lemma 4.1 that $\bar{n}^s$ is locally stable under admissible demand. It was also reported in the literature that the system state would remain unchanged under the very congested scenario because the inflow would always compensate for the outflow. Figure 6(b) depicts the state trajectory under *strictly admissible* travel demand with the same initial state and demand setting. The only difference is that the state trajectory triggered by the initial condition $n(0) = 8000$ (veh) will also converge. Because we can observe that this trajectory would first go to $\bar{n}^u$ and then move to $\bar{n}^s$ because the region of attraction of $\bar{n}^u$ has a zero radius under strictly admissible demand, i.e., $\bar{n}^u$ is no longer an equilibrium of the system. These results are intuitive that the available space will be filled by the demand if it is sufficiently large in a congested situation. If there is no boundary condition, the system state will tend to positive infinity which is not realistic. The boundary condition specified by the strictly admissible demand at the congested regime restricts the traffic entering the over-saturated region to an amount that is slightly less than the available space so that the system will not break down.
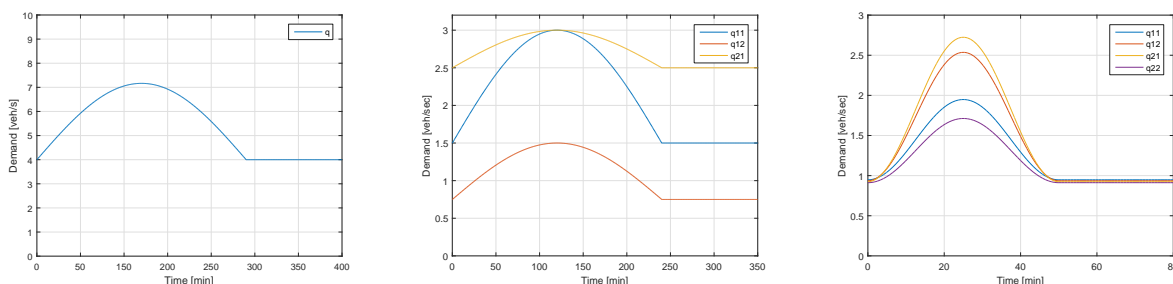
(a) For single-region MFD system without control

(b) For single-region MFD system with control

(c) For two-region MFD system

Figure 5: Time-varying travel demand patterns

A *time-varying demand* pattern as depicted in Figure 5(a) is used to simulate the time-varying nature of the demand pattern on the MFD system dynamics. The time-varying demand pattern is of the following form:

$$q(t) = \begin{cases} 4 + 3.165\sin(2\pi/480 \cdot t - 2\pi/240), & \text{if } 0 \le t \le 240 \\ 4, & \text{otherwise} \end{cases}$$

In this example, we adopt the method for converting alternating current (AC) sinusoidal voltage to direct current (DC) voltage in electrical engineering to define the steady state for the time-varying demand pattern. In line with this, two sets of steady states can be deduced from the steady state of travel demand with respect to different time spans, that is, peak and off-peak hours. For peak hours, $\bar{n}^s = 3000$ (veh); for off-peak hours, $\bar{n}^s = 1238$ (veh).

Figure 7(a) and Figure 7(b) depicts the state trajectories under *admissible* and *strictly admissible* travel demand with initial states starting from a free flow regime, e.g., $n(0) = 500, 1500, 2500$ (veh). We can observe from Figure 7(a) that the system trajectory would not evolve towards the first target equilibrium $\bar{n}^s = 3000$ (veh) because the steady state for the time-varying demand obtained from AC to DC voltage

22

conversion is not the true steady state for this demand pattern but a 'priori' of the traffic manager. Generally, a traffic manager would not be able to calibrate a functional form of a time-varying demand. Even if such a functional form is possible, it is difficult to infer the steady state. For the time-varying demand case, we discussed in Remark 4.2 that no uniform definition of the steady state of travel demand is recognized in the MFD literature. This renders identification of a steady state from a time-varying demand profile (especially for the fast time-varying case) a significantly difficult and unclear task in practice. When the steady state is well-defined, that is, the second part $\bar{n}^s = 1238$ (veh), the system trajectory converges to the desired equilibrium in line with Lemma 4.1 for the initial states less than $\bar{n}^u$ while is marginally stable for initial states above $\bar{n}^u$.

Although the traffic manager may have difficulties in calibrating a functional form and its steady state for the time-varying demand, he or she has a preferable network condition (or state) for management purposes. He or she can infer a stationary demand from the target network state and define it as a desired steady state for the time-varying demand. In this scenario, the *strictly admissible* travel demand furnishes a luxury degree of freedom that allows the traffic manager to enforce his or her 'priori' regardless of the true steady state (that is a 'miracle' to him or her) such that the management objective is attainable. The simulation results show that trajectories first converge to the equilibrium point $\bar{n}^s = 3000$ (veh) induced by the 'steady-state' demand of peak hours and then converge to the equilibrium point $\bar{n}^s = 1238$ (veh) induced by the steady-state demand of off-peak hours under *strictly admissible* travel demand in accordance with Lemma 4.1. This implies that for an MFD system with constant demand and time-varying demand, the equilibrium $\bar{n}^s$ is globally asymptotically stable under the *strictly admissible* travel demand, which is similar to the results of the CTM model in Gomes et al. (2008). This can be regarded as a superiority of the *strictly admissible* travel demand over the *admissible* travel demand in real-world practice (when the steady state is not available) but at the price of being less general in terms of mathematics. The strictly admissible demand can be regarded as a set of boundary conditions that restrict the traffic that enters the protected region to meet the management purpose without detailed information on the travel demand.
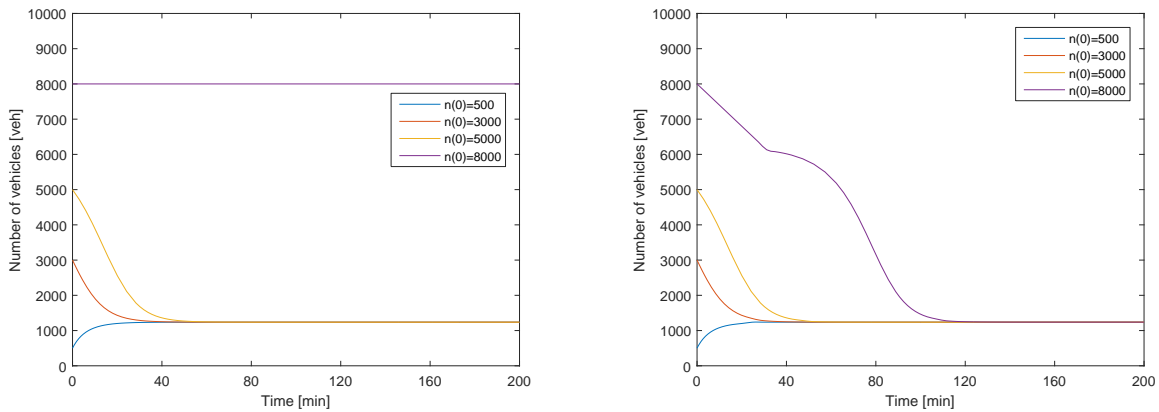
(a) State trajectories under admissible travel demand   (b) State trajectories under strictly admissible travel demand

Figure 6: State trajectories of single-region MFD system with constant demand and no control
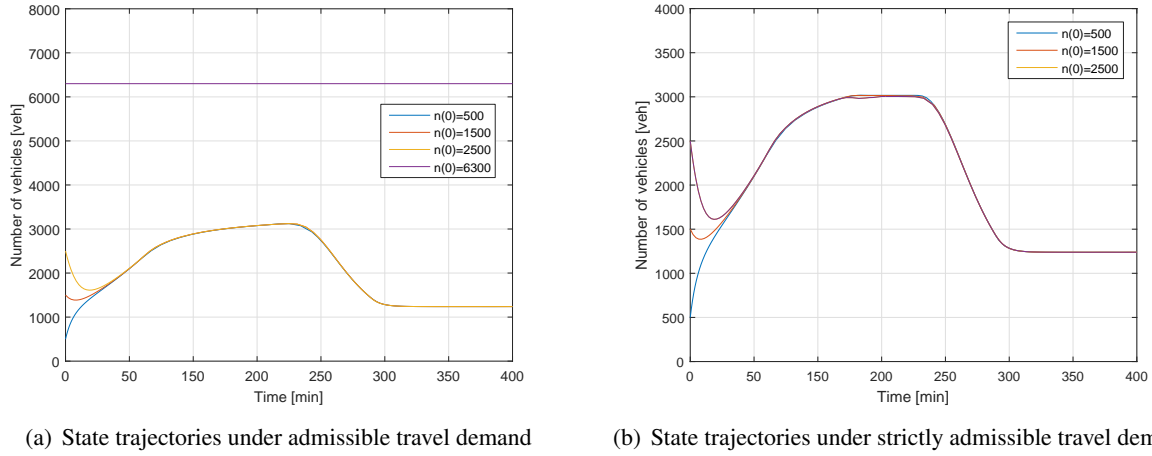
23

(a) State trajectories under admissible travel demand   (b) State trajectories under strictly admissible travel demand

Figure 7: State trajectories of single-region MFD system with time-varying demand and no control

5.2. Single-region MFD system with pricing control

In this case, we apply the proposed strictly admissible travel demand for the one-region MFD system with control to adjust the demand loaded into the region and to regulate the dynamics by the perimeter control. The demand patterns and network configurations are adopted from Haddad and Shraiber (2014), i.e., $[q_{11}, q_{12}, q_{21}] = [0.75, 1.5, 5]$ (veh/s); the initial accumulation is $n_1(0) = 7000$ (veh) and the equilibrium is set to be $\bar{n}_1 = 1000$ (veh). Figure 8(a) presents the evolution of network accumulation by choosing the perimeter control gain as the desired steady state of the ratio of the cross-boundary traffic in accordance to Corollary 4.2. It takes about 1500 s for the network accumulation to converge to the target equilibrium. This performance is similar to that of the Robust-PI controller proposed by Haddad and Shraiber (2014) wherein it takes about 1800 s for the network accumulation to converge to the target equilibrium under the same setting.

The following time-varying demand patterns as depicted in Figure 5(b) are used to simulate the morning peak,

$$[q_{11}(t),\ q_{12}(t),\ q_{21}(t)]^T = \begin{cases} \begin{bmatrix} 1.5 + 1.5\sin(\frac{2\pi}{480}t - \frac{2\pi}{240}) \\ 0.75 + 0.75\sin(\frac{2\pi}{480}t - \frac{2\pi}{240}) \\ 2.5 + 0.5\sin(\frac{2\pi}{480}t - \frac{2\pi}{240}) \end{bmatrix}, & \text{if } 0 \le t \le 240 \\ [1.5 \quad 0.75 \quad 2.5]^T, & \text{otherwise} \end{cases}$$

The initial accumulation is $n_1(0) = 7000$ (veh) and the equilibrium is set to be $\bar{n}_1 = 2000$ (veh). Figure 8(b) presents the evolution of state trajectories by choosing the steady-state control gain in accordance to Corollary 4.2. By specifying the VOT as 40 (CNY/h), a pricing scheme following (21) is obtained and depicted in Figure 8(c). As shown in Figure 8(c), when the initial network accumulation exceeds the target equilibrium whilst the demand keeps increasing as peak hour spans, the toll increases rapidly. The toll increment is to depress the network accumulation from over-saturation (with respect to the demand increment) and to regulate the network accumulation towards the target equilibrium. The toll then decreases in accordance to the decrease of demand pattern. Although the network accumulation n_1 enters its steady state at about 80 min, the partial states n_{11} and n_{12} are still evolving towards their steady states until 250 min. Since the toll is related to the partial states according to (21), it would attain the steady state only when all the states converge to their steady states as illustrated in Figure 8(b). After the network accumulation is brought down

24

and all the network accumulations (including n_1, n_{11} and n_{12}) reach the target equilibria, the toll achieves its steady state VOT $\cdot \frac{\bar{n}_1}{G_1(\bar{n}_1)}$.

(a) State trajectories under constant travel demand

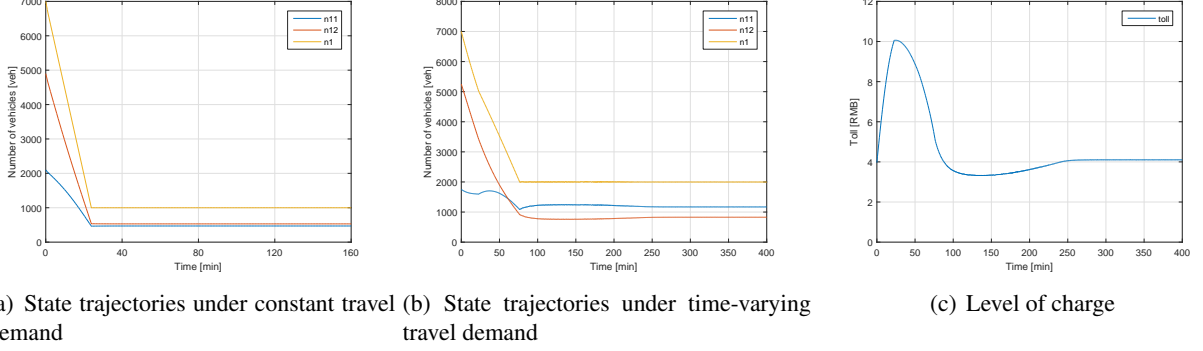(b) State trajectories under time-varying travel demand

(c) Level of charge

Figure 8: State trajectories and level of charge of single-region MFD system control

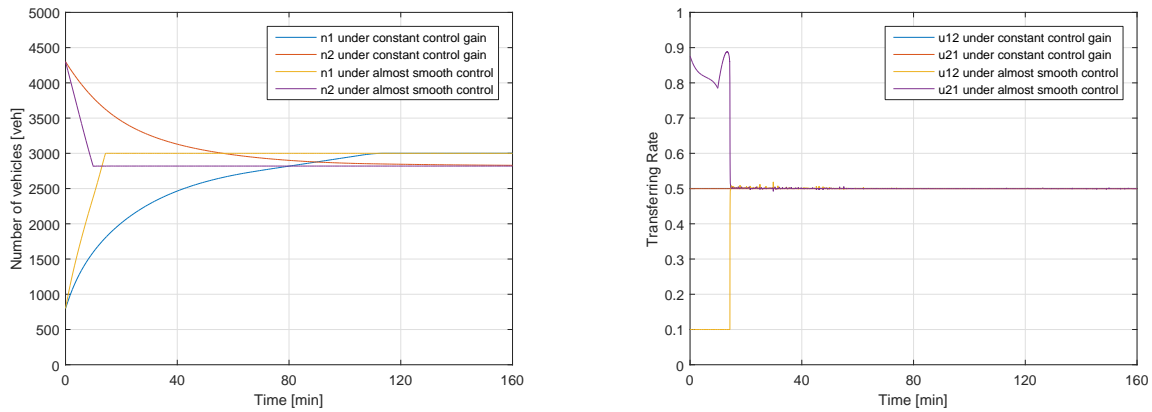### 5.3. Two-region MFD system with control

In this case, we apply the proposed strictly admissible travel demand of the two-region MFD system with control to adjust the demand loaded into the region and to regulate the system dynamics. The original demand pattern is assumed to be constant, $q = [1.58, 1.56, 1.54, 1.52]$ (veh/s); the initial accumulation state is randomly chosen as $n(0) = [800, 4300]$ (veh), split into four parts as $n_{11}(0) = 0.3n_1(0)$, $n_{12}(0) = 0.7n_1(0)$, $n_{21}(0) = 0.3n_2(0)$ and $n_{22}(0) = 0.7n_2(0)$. The equilibria induced by the steady-state travel demand are chosen as $\bar{n}_1^s = 3000$ (veh) and $\bar{n}_2^s = 2819$ (veh), and the corresponding four state equilibria are then $\bar{n} =$ [1500.5, 1499.5, 1410, 1409] (veh) and the corresponding controllers are $\bar{u} = [0.5003, 0.4997]$ by solving steady-state equations.

Given a constant control gain input as the steady state $\bar{u} = [0.5003, 0.4997]$, the state trajectories and control inputs are presented in Figure 9(a) and Figure 9(b), respectively. The simulation results show that under constant control gain, i.e., $u = [0.5003, 0.4997]$, the initial accumulation state $[n_1(0), n_2(0)] =$ [800, 4300] (veh) converges to the set equilibria $[\bar{n}_1^s, \bar{n}_2^s] = [3000, 2819]$ in line with Corollary 4.1 in more than 100 minutes. For a comparison, given the almost smooth feedback control as described in Appendix E (Zhong et al., 2017), the state trajectories and control inputs over time are depicted in Figure 9(a) and Figure 9(b) against the constant control gain case per Corollary 4.1. It is found that the accumulation states under almost smooth control converge much more quickly (less than 20 minutes) than the results in the constant control gain case. This indicates the merit of the dynamic control gain function over the constant one but at the price of complexity. There is always a trade-off between the complexity and efficiency according to the no free lunch theorem.

We also study the time-varying demand case for the two-region MFD system using the following demand pattern $q = \bar{q} + Q(t)$ as depicted in Figure 5(c), where $\bar{q} = [0.948, 0.936, 0.924, 0.912]^T$ (veh/s), and

$$Q(t) = \begin{cases} \begin{bmatrix} 0.5 + 0.5\sin(\frac{\pi}{25}t - \frac{\pi}{2}) \\ 0.8 + 0.8\sin(\frac{\pi}{25}t - \frac{\pi}{2}) \\ 0.9 + 0.9\sin(\frac{\pi}{25}t - \frac{\pi}{2}) \\ 0.4 + 0.4\sin(\frac{\pi}{25}t - \frac{\pi}{2}) \end{bmatrix}, & \text{if } 0 \le t \le 50 \\ [0 \ 0 \ 0 \ 0]^T, & \text{otherwise} \end{cases}$$

25

Given a constant control gain input as the steady state $\bar{u} = [0.2144, 0.2142]$, the state trajectories and control inputs are presented in Figure 10(a) and Figure 10(b), respectively, whilst the results under the feedback (almost smooth) control given by Zhong et al. (2017) are used for comparison. The simulation results show that under constant control gain, i.e., $u = [0.2144, 0.2142]$, the initial accumulation state $n_2(0) = 4300$ (veh) converges to the set equilibria $\bar{n}_2^s = 2819$ (veh) in accordance with Corollary 4.1 in more than 450 minutes, although $n_1(0) = 800$ (veh) converges to $\bar{n}_1^s = 3000$ (veh) in less than 30 minutes. It is noteworthy that the accumulation states under almost smooth control converge much more quickly (less than 30 minutes) than the results in the constant control gain case, which indicates the superiority of the dynamic control gain function over the constant one. Nevertheless, the constant control gain chosen as the steady state $\bar{u}$ can still be converted to a tolling scheme as discussed in Subsection 4.4 and guarantee the stability and convergence of the traffic dynamics to the desired equilibrium.

(a) State trajectories under constant control gain vs under almost smooth control

(b) Control inputs over time under constant control gain vs under almost smooth control

Figure 9: Constant travel demand of two region MFD system
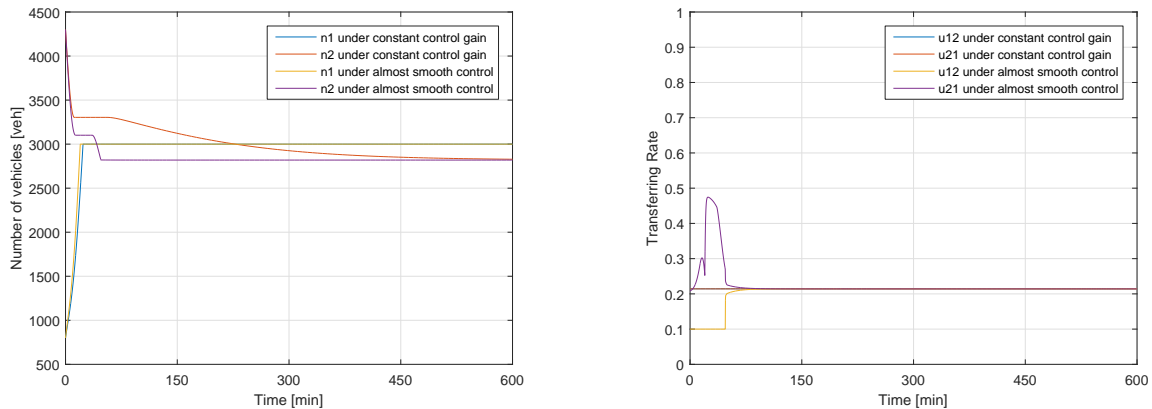
(a) State trajectories under constant control gain vs under almost smooth control

(b) Control inputs over time under constant control gain vs under almost smooth control

Figure 10: Time-varying demand of two-region MFD system

Furthermore, we assume the time-varying demand function is subject to an unbiased noise, i.e., $\xi(t) = [\xi_{11}(t), \xi_{12}(t), \xi_{21}(t), \xi_{22}(t)]^T$ with $\xi_{ij}(t) \sim N(0, 0.1)$ normally distributed while the MFD is subject to calibration errors as depicted in Figure 11(a). The settings are identical to that of the previous case except that additional MFD and demand uncertainties are introduced in the simulation. The constant perimeter control scheme implied by Corollary 4.1 and almost smooth control scheme adopted from Zhong et al. (2017) are applied to regulate the traffic dynamics to the desired equilibrium, respectively. As illustrated in Figure 11(b), the two-region MFD system can converge to the desired equilibria and is thus robustly stable in presence of both demand noise and MFD errors. Although the accumulation states under these three scenarios, i.e., without demand noise or MFD error (Figure 10(a)), with demand noise but no MFD error (Figure 11(b)), and with both demand noise and MFD error (Figure 11(b)), converge to the desired equilibrium, their transient behaviors are different. Generally speaking, more uncertain we are about the network environment, more control effort is needed to achieve the same objective since robustness is somehow at the price of a more conservative scheme. Interested readers are referred to Zhong et al. (2017) for a more detailed discussion on this. Compared with that under certain environment, it generally takes a longer time for the traffic state to converge to the desired equilibrium under uncertain scenarios.
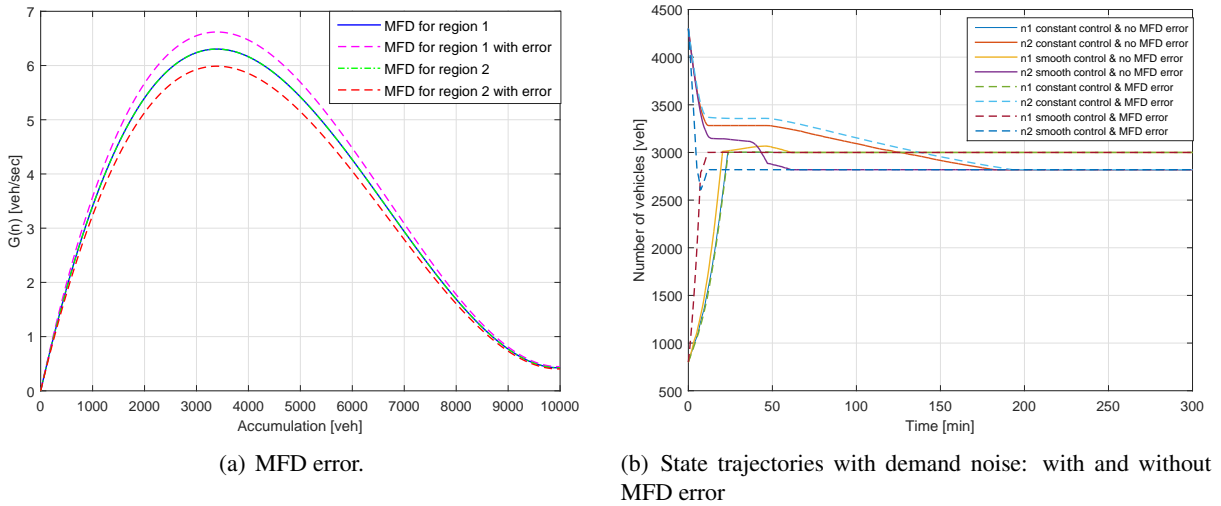

(a) MFD error.

(b) State trajectories with demand noise: with and without MFD error

Figure 11: Time-varying demand with MFD error and demand noise of two-region MFD system

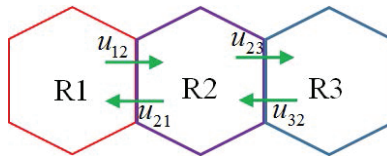### 5.4. Three-region MFD system with control

Figure 12: Three-region MFD system with control

The multi-region MFD system is rarely discussed in the literature. We apply the proposed strictly admissible travel demand of a three-region MFD system with control (as depicted in Figure 12) for demand adjustment to regulate the system dynamics in this case. R_1, R_2 and R_3 admit identical MFDs as defined by

27

(22). Assume a stationary demand pattern $[q_{11}, q_{12}, q_{21}, q_{22}, q_{23}, q_{32}, q_{33}] = [2, 1.3, 1.25, 1.2, 1.15, 1.05, 2.5]$ (veh/s) with the initial accumulation state randomly chosen as $[n_1(0), n_2(0), n_3(0)] = [800, 4300, 1500]$ (veh), and split into seven parts as $n_{11}(0) = 0.3n_1(0)$, $n_{12}(0) = 0.7n_1(0)$, $n_{21}(0) = 0.2n_2(0)$, $n_{22}(0) = 0.5n_2(0)$, $n_{23}(0) = 0.3n_2(0)$, $n_{32}(0) = 0.6n_3(0)$ and $n_{33}(0) = 0.4n_3(0)$. The target equilibria induced by the steady-state travel demand are $\bar{n}_1^s = \bar{n}_2^s = \bar{n}_3^s = 3000$ (veh). By solving steady-state equations, a set of feasible corresponding seven state equilibria and controllers are evaluated as $[\bar{n}_{11}, \bar{n}_{12}, \bar{n}_{21}, \bar{n}_{22}, \bar{n}_{23}, \bar{n}_{32}, \bar{n}_{33}] = [1563, 1437, 673, 1707, 620, 1004, 1996]$ (veh) and $[\bar{u}_{12}, \bar{u}_{21}, \bar{u}_{32}, \bar{u}_{23}] = [0.4351, 0.8928, 0.8928, 0.5029]$, respectively[3].

Given a constant control input as this steady state, the state trajectories are presented in Figure 13(a) and Figure 13(b), respectively. The centre region R_2 starts from the congested regime, $n_2(0) = 4300$ (veh), while the two periphery/adjacent regions R_1 and R_3 are in free-flow state, $[n_1(0), n_3(0)] = [800, 1500]$ (veh). The convergence of all the component accumulations to their desired equilibria in Figure 13(a) indicates that the constant perimeter controls balance the accumulation distribution among regions. Three accumulations accordingly converge to the desired states in about 120 minutes. This verifies Theorem 4.1 that the steady-state control in conjunction with the boundary condition specified by the strictly admissible demand per (16) can guarantee the global asymptotical stability of general multi-region MFD system.
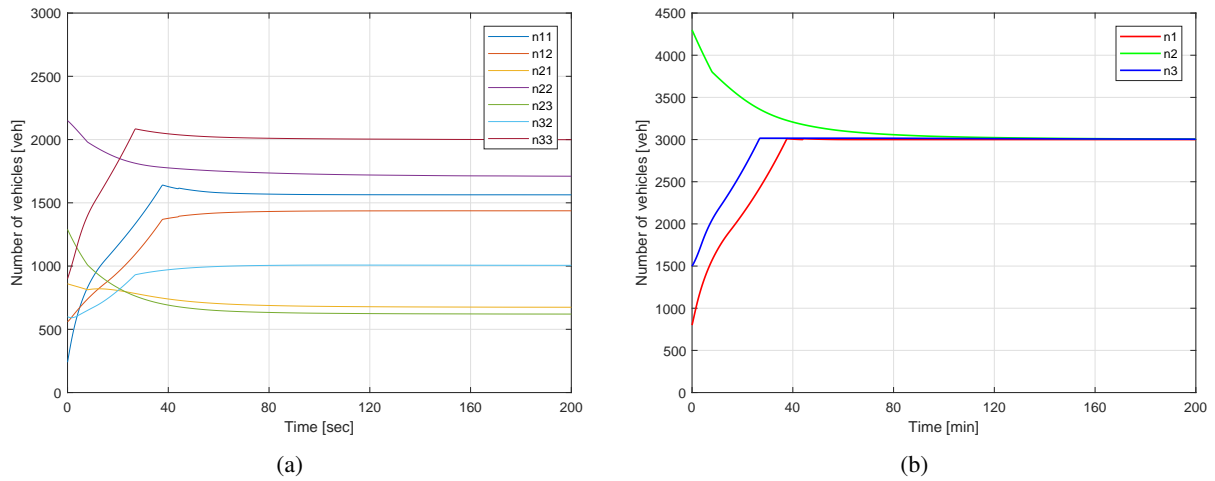

Figure 13: Three-region MFD system with constant control

6. Conclusions

The effects of the time-varying nature of travel demand on the behavior of MFD network traffic dynamics were investigated for the design of high-level control strategies such as perimeter (or gating) control and traffic rationing. Feasible demand concept was proposed to satisfy the necessary conditions for the solvability of steady-state equations and thus for the existence of equilibrium of general multi-region MFD systems. With the help of (strictly) admissible demand, a set of boundary conditions were devised to ensure the MFD dynamics were well-defined for a given demand pattern. For a single region without control, the boundary condition can be regarded as a travel demand adjustment scheme for traffic rationing. For the

---

[3] Detailed derivation for the three-region MFD system may be referred to the online appendix at https://www.dropbox.com/s/zrwvlrp6ook9yba/TRB_2017_32_onapp.pdf?dl=0.

case with perimeter (or gating) control, a set of sufficient conditions that guarantee the controllability, an important but yet untouched issue, were derived for general multi-region MFD systems. Given the cross-boundary travel demand, the traffic manager would determine the desired (amount of) steady state of the cross-boundary traffic from the steady-state equations. Under strictly admissible travel demand, it was verified that network traffic can converge to the desired uncongested equilibrium by suitable perimeter control gain function whose steady state equals the desired steady state of the ration of the cross-boundary traffic. This surprising finding indicates that the perimeter control gain function can be simply chosen as its desired steady state, that is, the control gain can be a constant and thus the control is a proportional control. The implication of this property to road pricing design based on the MFD framework was then discussed. Traffic rationing schemes can be implemented in line with the boundary conditions governed by the strictly admissible travel demand. The stability of the network equilibrium and convergence of the network dynamics were analyzed in the sense of Lyapunov. Both theoretical and numerical results indicate that the network traffic can converge to the desired uncongested equilibrium under various scenarios. The results are consistent with some existing studies. It offers a control systems perspective regarding the demand-oriented behavior analysis of MFD network traffic dynamics.

The steady state concept is rooted in transportation engineering. However, no clear definition of steady state for the time-varying travel demand and a traffic network exists in the literature. Therefore, defining the steady state of a time-varying demand pattern (especially for the fast time-varying case) remains a significantly difficult and interesting challenge, and thus a prospective direction for future work. The conditions regarding the controllability of the MFD system devised in this paper are sufficient only, and thus they may be conservative. The derivation of necessary conditions may be also a prospective direction for future work.

Acknowledgments

Appendix A. Derivation of steady-state equations and proof of necessary conditions for solvability

A.1. For single-region MFD system

This appendix presents the derivation of the steady state of $\bar{n}_{11}$, $\bar{n}_{12}$, $\bar{u}$. Denote $\bar{n}_1$, $\bar{u}$ and $\bar{q}_{11}$, $\bar{q}_{12}$, $\bar{q}_{21}$ as the steady states of the accumulation, controller and travel demands, respectively. Note that $\bar{n}_1 = \bar{n}_{11} + \bar{n}_{12}$, let $dn_{11}/dt = 0$ and $dn_{12}/dt = 0$, one gets

$$\bar{q}_{11} + (1 - \bar{u})\bar{q}_{21} = \frac{\bar{n}_{11}}{\bar{n}_1}G_1(\bar{n}_1) \tag{A.1a}$$

$$\bar{q}_{12} = \frac{\bar{n}_{12}}{\bar{n}_1}G_1(\bar{n}_1)\bar{u} \tag{A.1b}$$

i.e.,

$$\bar{n}_1[\bar{q}_{11} + (1 - \bar{u})\bar{q}_{21}] = \bar{n}_{11}G_1(\bar{n}_1) \tag{A.2a}$$

$$\bar{n}_1\bar{q}_{12} = \bar{n}_{12}G_1(\bar{n}_1)\bar{u} \tag{A.2b}$$

Dividing (A.2a) by (A.2b), one obtains

$$\frac{\bar{q}_{11} + (1 - \bar{u}\bar{q}_{21})}{\bar{q}_{12}} = \frac{\bar{n}_{11}}{\bar{n}_{12}\bar{u}}$$

We then get the following quadratic equation

$$
\begin{aligned}
& \bar{q}_{21}\bar{n}_{12}\bar{u}^2 - (\bar{q}_{11} + \bar{q}_{21})\bar{n}_{12}\bar{u} + \bar{n}_{11}\bar{q}_{12} = 0 \\
\Rightarrow \quad & \bar{q}_{21}\bar{u}^2 - (\bar{q}_{11} + \bar{q}_{21})\bar{u} + \frac{\bar{n}_{11}}{\bar{n}_{12}}\bar{q}_{12} = 0 \\
\Rightarrow \quad & \bar{q}_{21}\bar{u}^2 - [\bar{q}_{11} + \bar{q}_{21} - G_1(\bar{n}_1)]\bar{u} - G_1(\bar{n}_1)\bar{u} + \frac{\bar{n}_{11}}{\bar{n}_{12}}\bar{q}_{12} = 0
\end{aligned}
\tag{A.3}
$$

From (A.1b), we have

$$\bar{q}_{12} + \frac{\bar{n}_{11}}{\bar{n}_{12}}\bar{q}_{12} = G_1(\bar{n}_1)\bar{u} \tag{A.4}$$

In conjunction with (A.3) and (A.4), one gets

$$\bar{q}_{21}\bar{u}^2 - [\bar{q}_{11} + \bar{q}_{21} - G_1(\bar{n}_1)]\bar{u} - \bar{q}_{12} = 0 \tag{A.5}$$

Solving the quadratic equation (A.5), we obtain

$$\bar{u} = \frac{\bar{q}_{11} + \bar{q}_{21} - G_1(\bar{n}_1) \pm \sqrt{[\bar{q}_{11} + \bar{q}_{21} - G_1(\bar{n}_1)]^2 + 4\bar{q}_{12}\bar{q}_{21}}}{2\bar{q}_{21}} \tag{A.6}$$

Note that $\bar{q}_{11} + \bar{q}_{21} - G_1(\bar{n}_1) - \sqrt{[\bar{q}_{11} + \bar{q}_{21} - G_1(\bar{n}_1)]^2 + 4\bar{q}_{12}\bar{q}_{21}} \le 0$ implies that $\bar{u} \le 0$, thus there is only one admissible solution for $\bar{u}$, i.e.,

$$\bar{u} = \frac{\bar{q}_{11} + \bar{q}_{21} - G_1(\bar{n}_1) + \sqrt{[\bar{q}_{11} + \bar{q}_{21} - G_1(\bar{n}_1)]^2 + 4\bar{q}_{12}\bar{q}_{21}}}{2\bar{q}_{21}} \tag{A.7}$$

Let $\bar{u}$ be substituted by (A.7) in (A.1b), recalling $\bar{n}_1 = \bar{n}_{11} + \bar{n}_{12}$ one has

$$\bar{n}_{11} = \bar{n}_1 - \frac{2\bar{q}_{12}\bar{q}_{21}\bar{n}_1}{G_1(\bar{n}_1)[A + \sqrt{A^2 + 4\bar{q}_{12}\bar{q}_{21}}]}, \quad \bar{n}_{12} = \frac{2\bar{q}_{12}\bar{q}_{21}\bar{n}_1}{G_1(\bar{n}_1)[A + \sqrt{A^2 + 4\bar{q}_{12}\bar{q}_{21}}]}$$

where $A \triangleq \bar{q}_{11} + \bar{q}_{21} - G_1(\bar{n}_1)$.

A.2. For two-region MFD system

This appendix presents the derivation of the steady-state values of $\bar{n} = [\bar{n}_{11}, \bar{n}_{12}, \bar{n}_{21}, \bar{n}_{22}]^T$ and $\bar{u} = [\bar{u}_{12}, \bar{u}_{21}]^T$. With

$$\bar{n}_1 = \bar{n}_{11} + \bar{n}_{12}, \quad \bar{n}_2 = \bar{n}_{21} + \bar{n}_{22}, \quad \bar{q}_1 = \bar{q}_{11} + \bar{q}_{12}, \quad \bar{q}_2 = \bar{q}_{21} + \bar{q}_{22} \tag{A.8}$$

let $\mathrm{d}n_{11}/\mathrm{d}t = 0$, $\mathrm{d}n_{12}/\mathrm{d}t = 0$, $\mathrm{d}n_{21}/\mathrm{d}t = 0$, and $\mathrm{d}n_{22}/\mathrm{d}t = 0$, one obtains

$$0 = -\frac{\bar{n}_{11}}{\bar{n}_1}G_1(\bar{n}_1) + \frac{\bar{n}_{21}}{\bar{n}_2}G_2(\bar{n}_2)\bar{u}_{21} + \bar{q}_{11}, \quad 0 = -\frac{\bar{n}_{12}}{\bar{n}_1}G_1(\bar{n}_1)\bar{u}_{12} + \bar{q}_{12} \tag{A.9a}$$

$$0 = -\frac{\bar{n}_{22}}{\bar{n}_2}G_2(\bar{n}_2) + \frac{\bar{n}_{12}}{\bar{n}_1}G_1(\bar{n}_1)\bar{u}_{12} + \bar{q}_{22}, \quad 0 = -\frac{\bar{n}_{21}}{\bar{n}_2}G_2(\bar{n}_2)\bar{u}_{21} + \bar{q}_{21} \tag{A.9b}$$

We then sum the equations in (A.9a) and (A.9b), respectively, and get

$$0 = -\frac{\bar{n}_{11}}{\bar{n}_1}G_1(\bar{n}_1) + \bar{q}_{11} + \bar{q}_{21}, \quad 0 = -\frac{\bar{n}_{22}}{\bar{n}_2}G_2(\bar{n}_2) + \bar{q}_{12} + \bar{q}_{22}$$

In conjunction with (A.8), i.e., $\bar{n}_i = \bar{n}_{ii} + \bar{n}_{ij}$ where $i, j = 1, 2$, one gets

$$\bar{n}_{11} = \frac{\bar{n}_1(\bar{q}_{11} + \bar{q}_{21})}{G_1(\bar{n}_1)}, \quad \bar{n}_{12} = \bar{n}_1 \frac{G_1(\bar{n}_1) - (\bar{q}_{11} + \bar{q}_{21})}{G_1(\bar{n}_1)} \tag{A.10a}$$

$$\bar{n}_{22} = \frac{\bar{n}_2(\bar{q}_{12} + \bar{q}_{22})}{G_2(\bar{n}_2)}, \quad \bar{n}_{21} = \bar{n}_2 \frac{G_2(\bar{n}_2) - (\bar{q}_{12} + \bar{q}_{22})}{G_2(\bar{n}_2)} \tag{A.10b}$$

From (A.9a) and (A.9b), we obtain

$$\bar{u}_{12} = \frac{\bar{q}_{12}\bar{n}_1}{\bar{n}_{12}G_1(\bar{n}_1)} = \frac{\bar{q}_{12}}{G_1(\bar{n}_1) - \bar{q}_{21} - \bar{q}_{11}}, \quad \bar{u}_{21} = \frac{\bar{q}_{21}\bar{n}_2}{\bar{n}_{21}G_2(\bar{n}_2)} = \frac{\bar{q}_{21}}{G_2(\bar{n}_2) - \bar{q}_{12} - \bar{q}_{22}} \tag{A.11}$$

A.3. For multi-region MFD system

For the multi-region MFD system with perimeter control (1a)-(1b), with

$$\bar{n}_i = \bar{n}_{ii} + \sum_{j \in S_i} \bar{n}_{ij}, \quad \bar{q}_i = \bar{q}_{ii} + \sum_{j \in S_i} \bar{q}_{ij} \tag{A.12}$$

we have the following equations:

$$0 = -\frac{\bar{n}_{ii}}{\bar{n}_i}G_i(\bar{n}_i) + \sum_{j \in S_i} \frac{\bar{n}_{ji}}{\bar{n}_j}G_j(\bar{n}_j)\bar{u}_{ji} + \bar{q}_{ii} \tag{A.13a}$$

$$0 = -\frac{\bar{n}_{ij}}{\bar{n}_i}G_i(\bar{n}_i)\bar{u}_{ij} + \bar{q}_{ij} \tag{A.13b}$$

from the equilibrium conditions $\frac{dn_{ii}(t)}{dt} = 0$, $\frac{dn_{ij}(t)}{dt} = 0$.

Summing (A.13b) according to the cross-boundary exit and entry flows, respectively, yields

$$0 = -\sum_{j \in S_i} \frac{\bar{n}_{ij}}{\bar{n}_i}G_i(\bar{n}_i)\bar{u}_{ij} + \sum_{j \in S_i} \bar{q}_{ij} \tag{A.14a}$$

$$0 = -\sum_{j \in S_i} \frac{\bar{n}_{ji}}{\bar{n}_j}G_j(\bar{n}_j)\bar{u}_{ji} + \sum_{j \in S_i} \bar{q}_{ji} \tag{A.14b}$$

Summing (A.13a) and (A.14b), results in

$$0 = -\frac{\bar{n}_{ii}}{\bar{n}_i}G_i(\bar{n}_i) + \bar{q}_{ii} + \sum_{j \in S_i} \bar{q}_{ji}, \quad \bar{n}_{ii} = \frac{\bar{n}_i}{G_i(\bar{n}_i)} \cdot (\bar{q}_{ii} + \sum_{j \in S_i} \bar{q}_{ji}) \tag{A.15}$$

A feasible solution of $\bar{n}_{ij}$ and $\bar{u}_{ij}$ can be then obtained by solving (A.12), (A.13a)-(A.13b) and (A.15).

A.4. Proof of Proposition 3.1

This appendix presents the proof of Proposition 3.1.

PROOF OF PROPOSITION 3.1. The discussion is divided into four parts.
(i) For the single-region MFD system without control (5), denoting $\bar{n}$ as its equilibrium, we have

$$\bar{q} = G(\bar{n}) \leq G^{\text{max}}$$

(ii) For the single-region MFD system with perimeter control (3a)-(3b), referring to Appendix A.1, the steady state of the control input $\bar{u}$ can be solved from the following quadratic equation regarding $\bar{u}$:

$$\bar{q}_{21}\bar{u}^2 - [\bar{q}_{11} + \bar{q}_{21} - G_1(\bar{n}_1)]\bar{u} - \bar{q}_{12} = 0$$

Assume that the above equation admits (two) real-valued solutions, otherwise the steady-state equations admit no solution. It follows from (A.6) that there are two solutions for $\bar{u}$, but only the positive one is likely to be admissible. Considering the control constraint $0 \leq \bar{u} \leq 1$, let $g(\bar{u}) = \bar{q}_{21}\bar{u}^2 - [\bar{q}_{11} + \bar{q}_{21} - G_1(\bar{n}_1)]\bar{u} - \bar{q}_{12}$, its trajectory over $\bar{u}$ is shown in Figure A.14. Referring to Figure A.14, it is necessary that
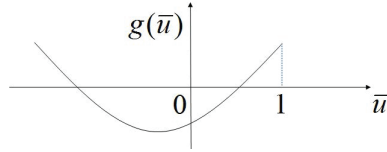

Figure A.14: The trajectory of $f(\bar{u})$.

$$g(0) \leq 0, \quad g(1) \geq 0.$$

It is trivial to show $g(0) = -\bar{q}_{12} \leq 0$. From $g(1) \geq 0$, we have

$$\bar{q}_{21} - [\bar{q}_{11} + \bar{q}_{21} - G_1(\bar{n}_1)] - \bar{q}_{12} \geq 0$$
$$\Rightarrow \quad -\bar{q}_{11} + G_1(\bar{n}_1) - \bar{q}_{12} \geq 0$$
$$\Rightarrow \quad \bar{q}_{11} + \bar{q}_{12} \leq G_1(\bar{n}_1)$$

(iii) For the four-state two-region MFD system with perimeter control (6a)-(6d), from (A.11), we have

$$\bar{n}_{12} = \frac{\bar{q}_{12}\bar{n}_1}{\bar{u}_{12}G_1(\bar{n}_1)}, \quad \bar{n}_{21} = \frac{\bar{q}_{21}\bar{n}_2}{\bar{u}_{21}G_2(\bar{n}_2)}. \tag{A.16}$$

Let $\bar{n}_{12}$ in (A.10a) and $\bar{n}_{21}$ in (A.10b) be substituted by (A.16) respectively, then

$$\frac{\bar{q}_{12}\bar{n}_1}{\bar{u}_{12}G_1(\bar{n}_1)} = \bar{n}_1 \frac{G_1(\bar{n}_1) - (\bar{q}_{11} + \bar{q}_{21})}{G_1(\bar{n}_1)}, \quad \frac{\bar{q}_{21}\bar{n}_2}{\bar{u}_{21}G_2(\bar{n}_2)} = \bar{n}_2 \frac{G_2(\bar{n}_2) - (\bar{q}_{12} + \bar{q}_{22})}{G_2(\bar{n}_2)}$$

It follows that

$$\bar{u}_{12} = \frac{\bar{q}_{21}}{G_1(\bar{n}_1) - (\bar{q}_{11} + \bar{q}_{21})}, \quad \bar{u}_{21} = \frac{\bar{q}_{12}}{G_2(\bar{n}_2) - (\bar{q}_{22} + \bar{q}_{12})}$$

32

Considering $\bar{u}_{12}, \bar{u}_{21} \in [0, 1]$, one gets

$$0 \le \frac{\bar{q}_{21}}{G_1(\bar{n}_1) - (\bar{q}_{11} + \bar{q}_{21})} \le 1, \quad 0 \le \frac{\bar{q}_{12}}{G_2(\bar{n}_2) - (\bar{q}_{22} + \bar{q}_{12})} \le 1$$

Then

$$\bar{q}_{11} + \bar{q}_{21} \le G_1(\bar{n}_1), \quad \bar{q}_{11} + \bar{q}_{12} + \bar{q}_{21} \le G_1(\bar{n}_1), \quad \bar{q}_{22} + \bar{q}_{12} \le G_2(\bar{n}_2), \quad \bar{q}_{22} + \bar{q}_{21} + \bar{q}_{12} \le G_2(\bar{n}_2)$$

i.e.,

$$\bar{q}_{11} + \bar{q}_{12} + \bar{q}_{21} \le G_1(\bar{n}_1), \quad \bar{q}_{22} + \bar{q}_{21} + \bar{q}_{12} \le G_2(\bar{n}_2)$$

(iv) For the multi-region MFD system with perimeter control (1a)-(1b) at steady state, from (A.15), we have

$$\bar{q}_{ii} + \sum_{j \in S_i} \bar{q}_{ji} = \frac{\bar{n}_{ii}}{\bar{n}_i} G_i(\bar{n}_i) \tag{A.17}$$

From (A.14a), considering $0 \le \bar{u}_{ij} \le 1$, one gets

$$\sum_{j \in S_i} \bar{q}_{ij} = \sum_{j \in S_i} \frac{\bar{n}_{ij}}{\bar{n}_i} G_i(\bar{n}_i) \bar{u}_{ij} \le \sum_{j \in S_i} G_i(\bar{n}_i) \cdot \frac{\bar{n}_{ij}}{\bar{n}_i} = (1 - \frac{\bar{n}_{ii}}{\bar{n}_i}) \cdot G_i(\bar{n}_i) \tag{A.18}$$

Summing (A.17) and (A.18) yields

$$\bar{q}_{ii} + \sum_{j \in S_i} \bar{q}_{ji} + \sum_{j \in S_i} \bar{q}_{ij} \le \frac{\bar{n}_{ii}}{\bar{n}_i} G_i(\bar{n}_i) + (1 - \frac{\bar{n}_{ii}}{\bar{n}_i}) \cdot G_i(\bar{n}_i) = G_i(\bar{n}_i)$$

■

Appendix B. Lyapunov theory

For a general nonlinear dynamic system:

$$\dot{\xi}(t) = f(\xi(t)), \quad \xi(t_0) = \xi_0 \tag{B.1}$$

where $\xi \in \mathbb{R}^n$, $t \in [t_0, \infty)$ and $f : \mathbb{R}^n \times \mathbb{R} \to \mathbb{R}^n$. ξ is called the state of the system, $\xi_0 \in \mathbb{R}^n$ the initial state and $t_0 \in \mathbb{R}$ the initial time. The components of ξ and f are denoted, respectively, by

$$\xi = \begin{bmatrix} \xi_1 \\ \vdots \\ \xi_n \end{bmatrix}, \quad f = \begin{bmatrix} f_1 \\ \vdots \\ f_n \end{bmatrix}.$$

Assume that $f : \mathbb{R}^n \times [t_0, \infty) \to \mathbb{R}^n$ is piecewise continuous in t and *locally Lipschitz* in ξ, i.e., there exists a constant L such that

$$\|f(\xi(t)) - f(\tilde{\xi}(t))\| \le L\|\xi - \tilde{\xi}\|$$

for all (ξ, t) and $(\tilde{\xi}, t)$ in some open neighborhood of (ξ_0, t_0). Under this assumption, given ξ_0, there exists some $t_1 > t_0$ and a unique continuous function $\xi : [t_0, t_1] \to \mathbb{R}^n$ that satisfies (B.1). This time function $\xi(t)$ is called a (local) solution of (B.1) over the interval $[t_0, t_1]$. The solution $\xi(t)$ is also called the state trajectory or simply the state of (B.1).

A constant vector $\xi_e \in \mathbb{R}^n$ is said to be an *equilibrium point* of the system (B.1) if $f(\xi_e) = 0, \ \forall t \geq t_0$.

If a nonzero vector ξ_e is an equilibrium point of (B.1), we can always introduce a new state variable $\bar{\xi} = \xi - \xi_e$ and define a new system $\dot{\bar{\xi}} = f(\bar{\xi} + \xi_e)$ that has $\bar{\xi} = 0$ as its equilibrium point. Thus, without loss of generality, we can always assume that the origin of $\mathbb{R}^n$ is an equilibrium point of the system (B.1). The following definitions regarding system stability refer to the equilibrium point of the origin.

Definition Appendix B.1. The equilibrium point $\xi_e = 0$ of the system (B.1) is

- Lyapunov stable if for any $\mathcal{R} > 0$, there exists a $r(\mathcal{R}) > 0$ such that, for all $\|\xi_0\| < r(\mathcal{R})$, $\|\xi(t)\| < \mathcal{R}$ for all $t \geq t_0$.
- unstable if it is not stable.
- asymptotically stable if it is stable, and there exists a $\delta > 0$ such that $\|\xi(t)\| \to 0$ as $t \to \infty$ for all $\|\xi_0\| < \delta$.
- globally asymptotically stable if it is stable and $\|\xi(t)\| \to 0$ as $t \to \infty$ for all $\xi_0 \in \mathbb{R}^n$. To our interest, we say the equilibrium point is globally asymptotically stable if it is stable and $\|\xi(t)\| \to 0$ as $t \to \infty$ for all ξ_0 in the feasible region.

∎

Definition Appendix B.2. Let $V : \mathbb{X} \to \mathbb{R}$ be a continuously differentiable function with $\mathbb{X}$ an open neighborhood of the origin of $\mathbb{R}^n$. V is said to be a (local) Lyapunov function of (B.1) if $V(\xi)$ is positive definite in $\mathbb{X}$, and

$$\dot{V}(\xi) \overset{def}{=} \sum_{i=1}^{n} \frac{\partial V}{\partial \xi_i} f_i(\xi) = \frac{\partial V}{\partial \xi} f(\xi)$$

is (locally) negative semi-definite. If $\mathbb{X} = \mathbb{R}^n$, and $\dot{V}(\xi)$ is negative semi-definite for all $\xi \in \mathbb{R}^n$, then $V(\xi)$ is said to be a global Lyapunov function for (B.1). ∎

Theorem Appendix B.1. If the system (B.1) has a Lyapunov function $V(\xi)$, then the equilibrium point $\xi_e = 0$ is Lyapunov stable. If, in addition, $\dot{V}(\xi)$ is locally negative definite in an open neighborhood of $\xi_e = 0$, then the equilibrium point $\xi_e = 0$ is asymptotically stable. ∎

Theorem Appendix B.2. Suppose that the system (B.1) has a global Lyapunov function $V(\xi)$, which is radially unbounded, i.e.,

$$\lim_{\|\xi\| \to \infty} V(\xi) = \infty$$

and, further, that $\dot{V}(\xi)$ is globally negative definite. The equilibrium point $\xi_e = 0$ is then globally asymptotically stable. ∎

Appendix C. Proof of Lemma 4.1

PROOF OF LEMMA 4.1. The uncongested and congested equilibria induced by a constant demand are per Theorem 3.1 and are depicted in Figure 3. Suppose $\bar{n}$ is an equilibrium of system (5), denote $\tilde{n} = n - \bar{n}$, it is trivial to prove that $V(\tilde{n}) = \frac{1}{2}\tilde{n}^2$ is continuously differentiable. Note that $V' = \tilde{n}$, one obtains

$$\inf \dot{V}(t) = \inf V'(\tilde{n})(\tilde{q} - G(n)) = \tilde{n}(\tilde{q} - G(n))$$

The proof of the first part of the Lemma can be deduced as:

For equilibrium $\bar{n}^s$, i.e., $\bar{n} = \bar{n}^s$, the following discussion is divided into four parts according to the accumulation n:

(i) Suppose $0 \le n < \bar{n}^s$, one gets $\tilde{n} = n - \bar{n}^s < 0$, and from (9), we have

$$\tilde{q} = \min\{q, G^{\max}\} = q > G(n) \Rightarrow \frac{d\tilde{n}}{dt} = q - G(n) > 0$$

Then $\dot{V} = \tilde{n}(\tilde{q} - G(n)) < 0$.

(ii) Suppose $\bar{n}^s \le n \le n_{cr}$, one gets $\tilde{n} = n - \bar{n}^s \ge 0$, and from (9), we have

$$\tilde{q} = \min\{q, G^{\max}\} = q < G(n) \Rightarrow \frac{d\tilde{n}}{dt} = q - G(n) \le 0$$

Then $\dot{V} = \tilde{n}(\tilde{q} - G(n)) \le 0$. And, $\dot{V} = 0$ if and only if $\tilde{n} = n - \bar{n}^s = 0$ or $\tilde{q} - G(n) = 0$, which both imply $n = \bar{n}^s$ as $n = \bar{n}^u$ is excluded from this interval.

(iii) Suppose $n_{cr} < n < \bar{n}^u$, one gets $\tilde{n} = n - \bar{n}^s > 0$, and from (9), we have

$$\tilde{q} = \min\{q, G(n)\} = q < G(n) \Rightarrow \frac{d\tilde{n}}{dt} = q - G(n) < 0$$

Then $\dot{V} = \tilde{n}(\tilde{q} - G(n)) < 0$.

(iv) Suppose $\bar{n}^u \le n < n_{jam}$, one gets $\tilde{n} = n - \bar{n}^s > 0$, and from (9), we have

$$\tilde{q} = \min\{q, G(n)\} = G(n) \Rightarrow \frac{d\tilde{n}}{dt} = G(n) - G(n) = 0$$

Then $\dot{V} = \tilde{n}(\tilde{q} - G(n)) = 0$. This implies that the accumulation stays at its initial state.

To sum up, there exists a continuously differentiable function $V(\tilde{n}) = \frac{1}{2}\tilde{n}^2$ such that

$$\begin{cases} V(0) = 0, \\ V(\tilde{n}) > 0, & \tilde{n} \in [0, \bar{n}_u), \quad \tilde{n} \ne 0 \\ V'(\tilde{n})(\tilde{q} - G(n)) \le 0, & \tilde{n} \in [0, \bar{n}_u) \end{cases}$$

Therefore, under the admissible demand per (9), the equilibrium $\bar{n}^s$ is locally Lyapunov stable. In addition, we have

$$V'(\tilde{n})(\tilde{q} - G(n)) < 0, \quad \tilde{n} \in [0, \bar{n}_u), \quad \tilde{n} \ne 0$$

Then the zero solution equilibrium $\bar{n}^s$ to $\dot{n} = \tilde{q} - G(n)$ is asymptotically stable.

Similar analysis can be established for equilibrium $\bar{n}^u$, i.e., $\bar{n} = \bar{n}^u$ and $\tilde{n} = n - \bar{n}^u$. As previously proven, all state trajectories with initial conditions in $[0, \bar{n}^u)$ will be attracted by $\bar{n}^s$. Therefore, we need only consider the state trajectory with an initial condition in $[\bar{n}^u, n_{jam})$.

Suppose $\bar{n}^u < n < n_{jam}$, one gets $\tilde{n} = n - \bar{n}^u > 0$, and from (9), we have

$$\tilde{q} = \min\{q, G(n)\} = G(n) \Rightarrow \frac{\mathrm{d}\tilde{n}}{\mathrm{d}t} = G(n) - G(n) = 0$$

Then $\dot{V} = \tilde{n}(\tilde{q} - G(n)) = 0$. Therefore, $\dot{V} = \tilde{n}(\tilde{q} - G(n)) = 0$, $\forall n \in [\bar{n}^u, n_{jam})$. This implies that the accumulation variable remains at its initial state, i.e., $\bar{n}^u$ is an unstable equilibrium.

For the special case in which $\bar{q} = G^{\max}$, it is feasible if and only if $n(0) = 0$, then $\bar{n}^s = \bar{n}^u = n_{cr}$. One gets $\tilde{n} = n - \bar{n}^s < 0$, and from (9), we have

$$\tilde{q} = \min\{\bar{q}, G^{\max}\} = G^{\max} \Rightarrow \frac{\mathrm{d}\tilde{n}}{\mathrm{d}t} = G^{\max} - G(n) > 0$$

Then $\dot{V} = \tilde{n}(\tilde{q} - G(n)) < 0$.

For equilibrium $\bar{n}^s$, $\forall n \in [0, \bar{n}^u)$, $\dot{V} < 0$, which implies that the trajectory converges to $\bar{n}^s$; $\forall n \in [\bar{n}^u, n_{jam})$, $\dot{V} = 0$, which implies the state trajectory remains at its initial value with admissible travel demand.

The proof of the second part of the Lemma can be deduced as:

Remind that under strictly feasible demand case, $\bar{n}^s$ is the unique equilibrium. The second part of the Lemma can be similarly proven. The difference lies in the $[\bar{n}^u, n_{jam})$. To be specific, suppose $\bar{n}^u \le n < n_{jam}$, one gets $\tilde{n} = n - \bar{n}^s > 0$, from Definition 4.2, we have

$$\tilde{q} = \min\{q, G(n) - \epsilon\} = G(n) - \epsilon < G(n) \Rightarrow \frac{\mathrm{d}\tilde{n}}{\mathrm{d}t} = G(n) - \epsilon - G(n) = -\epsilon < 0$$

then $\dot{V} = \tilde{n}(\tilde{q} - G(n)) < 0$.

Then for equilibrium $\bar{n}^s$, $\forall n \in [0, n_{jam})$, $\dot{V} < 0, \tilde{n} \ne 0$, i.e., $n \ne \bar{n}^s$, which implies the trajectory all converges to $\bar{n}^s$ with strictly admissible travel demand. ∎

Appendix D. Proof of Corollary 4.2

PROOF OF COROLLARY 4.2. Again, it is easy to show that $V(\tilde{n}_1) = \frac{1}{2}\tilde{n}_1^2$ is positive-definite, continuously differentiable and radially unbounded. To verify (17) holds, we evaluate the time derivative of $V(\tilde{n}_1)$.

$$\begin{aligned}
\inf_{\tilde{u} \in \mathcal{K}} \dot{V}(t) &= \inf_{\tilde{u} \in \mathcal{K}} V'(\tilde{n}_1)\dot{\tilde{n}}_1 = \tilde{n}_1 \frac{\mathrm{d}\tilde{n}_1}{\mathrm{d}t} = \tilde{n}_1 \frac{\mathrm{d}n_1}{\mathrm{d}t} \\
&= \tilde{n}_1 \Big[\tilde{q}(t) + q_{21}(t) - \upsilon(t)G_1\big(\tilde{n}_1(t) + \bar{n}_1^s\big) - \big(q_{21}(t) + (1 - \upsilon(t))G_1\big(\tilde{n}_1(t) + \bar{n}_1^s\big)\big)\big(\tilde{u}(t) + \bar{u}\big)\Big] \\
&= \tilde{n}_1 \Big\{ \tilde{q}(t) - G_1(\tilde{n}_1(t) + \bar{n}_1^s) - \Big[q_{21}(t) + \big(1 - \upsilon(t)\big)G_1\big(\tilde{n}_1(t) + \bar{n}_1^s\big)\Big]\big(1 - (\tilde{u}(t) + \bar{u})\big)\Big\} \\
&= \tilde{n}_1 \Big[-\big(G_1(n_1(t)) - \big(q_{21}(t) + (1 - \upsilon(t))G_1(n_1(t))\big)\big(1 - u(t)\big)\big) + \tilde{q}(t)\Big]
\end{aligned}$$

(i) Suppose $0 \le n_1 < \bar{n}_1^s$, one gets $\tilde{n}_1 < 0$. From (14), note that $G_1(n_1) \ge G_1(n_1) - \big[q_{21}(t) + (1 - \upsilon(t))G_1(n_1)\big]\big(1 - u(t)\big) + \epsilon_1$, the forthcoming discussion of this fold comprises three cases.

First, if $q(t) \le G_1(n_1) - \big[q_{21}(t) + (1 - \upsilon(t))G_1(n_1)\big]\big(1 - u(t)\big) + \epsilon_1 \le G_1(n_1)$, then

$$\tilde{q}(t) = G_1(n_1) - \big[q_{21}(t) + (1 - \upsilon(t))G_1(n_1)\big]\big(1 - u(t)\big) + \epsilon_1$$

36

It follows

$$V'(\tilde{n}_1)\dot{n}_1 = \tilde{n}_1\dot{n}_1$$

$$= \tilde{n}_1\left\{ G_1(n_1) - \left(q_{21}(t) + (1-\upsilon(t))G_1(n_1)\right)\left(1-u(t)\right) + \epsilon_1 - \left[G_1(n_1) - \left(q_{21}(t) + \left(1-\upsilon(t)\right)G_1(n_1)\right)\left(1-u(t)\right)\right]\right\}$$

$$= \tilde{n}_1\epsilon_1 < 0$$

If $G_1(n_1) - \left(q_{21}(t) + (1-\upsilon(t))G_1(n_1)\right)\left(1-u(t)\right) + \epsilon_1 \leq q(t) \leq G_1(n_1)$, then $\tilde{q}(t) = q(t)$. Thus

$$\dot{n}_1 = \tilde{q}(t) - \left[G_1(n_1) - \left(q_{21}(t) + (1-\upsilon(t))G_1(n_1)\right)\left(1-u(t)\right)\right]$$

$$= q(t) - \left[G_1(n_1) - \left(q_{21}(t) + (1-\upsilon(t))G_1(n_1)\right)\left(1-u(t)\right)\right]$$

$$\geq G_1(n_1) - \left(q_{21}(t) + (1-\upsilon(t))G_1(n_1)\right)\left(1-u(t)\right) + \epsilon_1 - \left[G_1(n_1) - \left(q_{21}(t) + (1-\upsilon(t))G_1(n_1)\right)\left(1-u(t)\right)\right]$$

$$= \epsilon_1 > 0$$

It follows $V'(\tilde{n}_1)\dot{n}_1 = \tilde{n}_1\dot{n}_1 < 0$.

If instead $G_1(n_1) - \left(q_{21}(t) + (1-\upsilon(t))G_1(n_1)\right)\left(1-u(t)\right) + \epsilon_1 \leq G_1(n_1) \leq q(t)$, then $\tilde{q}(t) = G_1(n_1)$. Thus

$$\dot{n}_1 = \tilde{q}(t) - \left[G_1(n_1) - \left(q_{21}(t) + (1-\upsilon(t))G_1(n_1)\right)\left(1-u(t)\right)\right]\left(1-u(t)\right)$$

$$= G_1(n_1) - \left[G_1(n_1) - \left(q_{21}(t) + (1-\upsilon(t))G_1(n_1)\right)\left(1-u(t)\right)\right]$$

$$= \left(q_{21}(t) + (1-\upsilon(t))G_1(n_1)\right)\left(1-u(t)\right) > 0$$

It follows $V'(\tilde{n}_1)\dot{n}_1 = \tilde{n}_1\dot{n}_1 < 0$.

(ii) Suppose $\bar{n}_1^s \leq n_1 < \bar{n}_1^u$, one gets $\tilde{n}_1 > 0$. From (14), we have

$$\tilde{q}(t) \leq G_1(n_1) - \left(q_{21}(t) + (1-\upsilon(t))G_1(n_1)\right)\left(1-u(t)\right)$$

$$\Rightarrow \quad \dot{n}_1 = \tilde{q}(t) - \left[G_1(n_1) - \left(q_{21}(t) + (1-\upsilon(t))G_1(n_1)\right)\left(1-u(t)\right)\right] \leq 0$$

Thus $V'(\tilde{n}_1)\dot{n}_1 = \tilde{n}_1\dot{n}_1 \leq 0$ and $V'(\tilde{n}_1)\dot{n}_1 = 0$ if and only if $\tilde{n}_1 = 0$, i.e., $n_1 = \bar{n}_1^s$.

(iii) Suppose $\bar{n}_1^u \leq n_1 < n_{1,jam}$, one gets $\tilde{n}_1 > 0$. From (14), we have

$$\tilde{q}(t) \leq G_1(n_1) - \left(q_{21}(t) + (1-\upsilon(t))G_1(n_1)\right)\left(1-u(t)\right) - \epsilon_2$$

$$\Rightarrow \quad \dot{n}_1 = \tilde{q}(t) - \left[G_1(n_1) - \left(q_{21}(t) + (1-\upsilon(t))G_1(n_1)\right)\left(1-u(t)\right)\right]$$

$$\leq G_1(n_1) - \left(q_{21}(t) + (1-\upsilon(t))G_1(n_1)\right)\left(1-u(t)\right) - \epsilon_2 - \left[G_1(n_1) - \left(q_{21}(t) + (1-\upsilon(t))G_1(n_1)\right)\left(1-u(t)\right)\right]$$

$$= -\epsilon_2 < 0$$

Thus $V'(\tilde{n}_1)\dot{n}_1 = \tilde{n}_1\dot{n}_1 < 0$.

To sum up, $\tilde{n}_1$ and $\dot{n}_1$ have opposite signs while $\tilde{n}_1 \neq 0$, i.e., $\tilde{n}_1 < 0$ (> 0) as long as $\dot{n}_1 > 0$ (< 0), thus

$$\tilde{n}_1\dot{n}_1 < 0,$$

whenever $\tilde{n}_1 \neq 0$. Therefore, $V'(\tilde{n}_1)\dot{\tilde{n}}_1 < 0$ when $\tilde{n}_1 \neq 0$.

For the case $V'(\tilde{n}_1) = 0$ while $\tilde{n}_1 = 0$. So obviously $V'(\tilde{n}_1)\dot{\tilde{n}}_1 = 0$ if $\tilde{n}_1 = 0$, i.e., $n_1 = \bar{n}_1^s$, then one gets

$$V'(\tilde{n}_1)\dot{\tilde{n}}_1 = \begin{cases} \tilde{n}_1\dot{n}_1 < 0, & \tilde{n}_1 \neq 0 \\ 0, & \tilde{n}_1 = 0 \end{cases}$$

That is, the function $V(\tilde{n}_1) = \frac{1}{2}\tilde{n}_1^2$, satisfying (17), is a CLF for system (4), which guarantees the system global stabilizability, with $\bar{n}_1^s$ as the globally asymptotically stable equilibrium. ∎

Appendix E. Dynamic feedback controller construction

As discussed in Section 4, if the equilibrium is not 0, it is a common practice to incorporate a coordinate transformation to convert the nontrivial equilibrium to the origin. Regarding the two-region MFD system (8a)-(8b), by introducing $\tilde{n} = n(t) - \bar{n}^s$ and $\tilde{u} = u(t) - \bar{u}$, it can be converted into an affine form

$$\dot{\tilde{n}} = F(\tilde{n}, \tilde{q}) + S(\tilde{n})\tilde{u} \tag{E.1}$$

where $\tilde{n}(t) = [\tilde{n}_1(t), \tilde{n}_2(t)]^T$, $\tilde{u}(t) = [\tilde{u}_{12}(t), \tilde{u}_{21}(t)]^T$, and

$$F \triangleq \left[\begin{array}{c} -v_{11}G_1(\tilde{n}_1 + \bar{n}_1^s) - v_{12}G_1(\tilde{n}_1 + \bar{n}_1^s)\bar{u}_{12} + v_{21}G_2(\tilde{n}_2 + \bar{n}_2^s)\bar{u}_{21} + \tilde{q}_1 \\ -v_{22}G_2(\tilde{n}_2 + \bar{n}_2^s) - v_{21}G_2(\tilde{n}_2 + \bar{n}_2^s)\bar{u}_{21} + v_{12}G_1(\tilde{n}_1 + \bar{n}_1^s)\bar{u}_{12} + \tilde{q}_2 \end{array} \right]$$

$$S \triangleq \left[\begin{array}{cc} -v_{12}G_1(\tilde{n}_1 + \bar{n}_1^s) & v_{21}G_2(\tilde{n}_2 + \bar{n}_2^s) \\ v_{12}G_1(\tilde{n}_1 + \bar{n}_1^s) & -v_{21}G_2(\tilde{n}_2 + \bar{n}_2^s) \end{array} \right]$$

Lemma Appendix E.1. Zhong et al. (2017) For the affine MFD system (E.1), an explicit dynamic feedback controller can be constructed as:

$$\tilde{u}(t) = \Phi\tilde{n}(t)) = \phi(\alpha(\tilde{n}), \|\beta(\tilde{n})\|^2)\beta(\tilde{n}) \tag{E.2}$$

$$\phi(\alpha(\tilde{n}), \|\beta(\tilde{n})\|^2) \triangleq \begin{cases} -\dfrac{\alpha(\tilde{n}) + \sqrt{\alpha^2(\tilde{n}) + (\beta^T(\tilde{n})\beta(\tilde{n}))^2}}{\beta^T(\tilde{n})\beta(\tilde{n})(1 + \sqrt{1 + \beta^T(\tilde{n})\beta(\tilde{n})})}, & \text{if } \beta(\tilde{n}) \neq 0 \\ 0, & \text{if } \beta(\tilde{n}) = 0 \end{cases}$$

where $V(\cdot)$ is a CLF, $\alpha(\tilde{n}) \triangleq V'(\tilde{n})F(\tilde{n}, q)$, $\beta(\tilde{n}) = [\beta_1(\tilde{n}), \ldots, \beta_k(\tilde{n})] \triangleq S^T(\tilde{n})V'^T(\tilde{n})$. ∎

References

Aboudolas, K. and Geroliminis, N., 2013. Perimeter and boundary flow control in multi-reservoir heterogeneous networks. *Transportation Research Part B: Methodological*, 55:265–281.

Daganzo, C. F., 1995. The cell transmission model, part II: Network traffic. *Transportation Research Part B: Methodological*, 29 (2):79–93.

Daganzo, C. F., 2007. Urban gridlock: Macroscopic modeling and mitigation approaches. *Transportation Research Part B: Methodological*, 41(1):49–62.

Daganzo, C. F., Gayah, V. V., and Gonzales, E. J., 2011. Macroscopic relations of urban traffic variables: Bifurcations, multivaluedness and instability. *Transportation Research Part B: Methodological*, 45(1):278–288.

Gayah, V. V. and Daganzo, C. F., 2011. Clockwise hysteresis loops in the macroscopic fundamental diagram: An effect of network instability. *Transportation Research Part B: Methodological*, 45(4):643–655.

Geng, N., Zhao, X., Xie, D., Li, X., and Gao, Z., 2015. Congestion mechanism and demand adjustment strategies for double-cell system with bottlenecks. *Transportation Research Part C: Emerging Technologies*, 57:122–145.

Geroliminis, N. and Daganzo, C. F., 2008. Existence of urban-scale macroscopic fundamental diagrams: Some experimental findings. *Transportation Research Part B: Methodological*, 42(9):759–770.

Geroliminis, N. and Sun, J., 2011. Hysteresis phenomena of a macroscopic fundamental diagram in freeway networks. *Transportation Research Part A: Policy and Practice*, 45(9):966–979.

Geroliminis, N., Haddad, J., and Ramezani, M., 2013. Optimal perimeter control for two urban regions with macroscopic fundamental diagrams: A model predictive approach. *IEEE Transactions on Intelligent Transportation Systems*, 14(1):348–359.

Godfrey, J. W., 1969. The mechanism of a road network. *Traffic Engineering and Control*, 11:323–327.

Gomes, G., Horowitz, R., Kurzhanskiy, A. A., Varaiya, P., and Kwon, J., 2008. Behavior of the cell transmission model and effectiveness of ramp metering. *Transportation Research Part C: Emerging Technologies*, 16(4):485–513.

Haddad, J., 2015. Robust constrained control of uncertain macroscopic fundamental diagram networks. *Transportation Research Part C: Emerging Technologies*, 59:323–339.

Haddad, J., 2017. Optimal coupled and decoupled perimeter control in one-region cities. *Control Engineering Practice*, 61: 134–148.

Haddad, J. and Geroliminis, N., 2012. On the stability of traffic perimeter control in two-region urban cities. *Transportation Research Part B: Methodological*, 46(9):1159–1176.

Haddad, J. and Mirkin, B., 2016. Adaptive perimeter traffic control of urban road networks based on MFD model with time delays. *International Journal of Robust and Nonlinear Control*, 26(6):1267–1285.

Haddad, J. and Shraiber, A., 2014. Robust perimeter control design for an urban region. *Transportation Research Part B: Methodological*, 68:315–332.

Haddad, J., Ramezani, M., and Geroliminis, N., 2013. Cooperative traffic control of a mixed network with two urban regions and a freeway. *Transportation Research Part B: Methodological*, 54:17–36.

Haddad, W. M. and Chellaboina, V., 2008. *Nonlinear dynamical systems and control: A Lyapunov-based approach*. Princeton University Press.

Jin, W. L., Gan, Q. J., and Gayah, V. V., 2013. A kinematic wave approach to traffic statics and dynamics in a double-ring network. *Transportation Research Part B: Methodological*, 57:114–131.

Keyvan-Ekbatani, M., Papageorgiou, M., and Papamichail, I., 2013. Urban congestion gating control based on reduced operational network fundamental diagrams. *Transportation Research Part C: Emerging Technologies*, 33:74–87.

Khalil, H., 2002. *Nonlinear Systems*. Prentice Hall, New Jersey., 3rd edition.

Knoop, V., Hoogendoorn, S., and Van Lint, J., 2012. Routing strategies based on macroscopic fundamental diagram. *Transportation Research Record*, (2315):1–10.

Kouvelas, A., Saeedmanesh, M., and Geroliminis, N., 2015. Feedback perimeter control for heterogeneous urban networks using adaptive optimization. In *Intelligent Transportation Systems (ITSC), 2015 IEEE 18th International Conference on*, pages 882–887. IEEE.

Kouvelas, A., Saeedmanesh, M., and Geroliminis, N., 2017. Enhancing model-based feedback perimeter control with data-driven online adaptive optimization. *Transportation Research Part B: Methodological*, 96:26–45.

Leclercq, L. and Geroliminis, N., 2013. Estimating MFDs in simple networks with route choice. *Transportation Research Part B: Methodological*, 57(7):468–484.

Leclercq, L., Chiabaut, N., and Trinquier, B., 2014. Macroscopic fundamental diagrams: A cross-comparison of estimation methods. *Transportation Research Part B: Methodological*, 62:1–12.

Leclercq, L., Sénécat, A., and Mariotte, G., 2017. Dynamic macroscopic simulation of on-street parking search: A trip-based approach. *Transportation Research Part B: Methodological*, 101:268–282.

Mahmassani, H. S., Saberi, M., and Zockaie, A., 2013. Urban network gridlock: Theory, characteristics, and dynamics. *Transportation Research Part C: Emerging Technologies*, 36:480–497.

Mazloumian, A., Geroliminis, N., and Helbing, D., 2010. The spatial variability of vehicle densities as determinant of urban network capacity. *Philosophical Transactions of the Royal Society A*, 368(1928):4627–4647.

Muñoz, L., Sun, X., Sun, D., Gomes, G., and Horowitz, R., 2004. Methodological calibration of the cell transmission model. In *American Control Conference, 2004. Proceedings of the 2004*, volume 1, pages 798–803. IEEE.

Ogata, K., 2010. *Modern control engineering*. Prentice Hall, New Jersey., 5th edition.

Ramezani, M., Haddad, J., and Geroliminis, N., 2015. Dynamics of heterogeneity in urban networks: aggregated traffic modeling and hierarchical control. *Transportation Research Part B: Methodological*, 74:1–19.

Saeedmanesh, M. and Geroliminis, N., 2017. Dynamic clustering and propagation of congestion in heterogeneously congested urban traffic networks. *Transportation Research Part B: Methodological*, 105:193–211.

Simoni, M., Pel, A., Waraich, R., and Hoogendoorn, S., 2015. Marginal cost congestion pricing based on the network fundamental diagram. *Transportation Research Part C: Emerging Technologies*, 56:221–238.

Yang, H. and Wang, X., 2011. Managing network mobility with tradable credits. *Transportation Research Part B: Methodological*, 45(3):580–594.

Yildirimoglu, M. and Geroliminis, N., 2014. Approximating dynamic equilibrium conditions with macroscopic fundamental diagrams. *Transportation Research Part B: Methodological*, 70:186–200.

Zhang, L., Garoni, T. M., and de Gier, J., 2013. A comparative study of macroscopic fundamental diagrams of arterial road networks governed by adaptive traffic signal systems. *Transportation Research Part B: Methodological*, 49:1–23.

Zheng, N., Waraich, R. A., Axhausen, K. W., and Geroliminis, N., 2012. A dynamic cordon pricing scheme combining the macroscopic fundamental diagram and an agent-based traffic model. *Transportation Research Part A: Policy and Practice*, 46(8):1291–1303.

Zheng, N., Rérat, G., and Geroliminis, N., 2016. Time-dependent area-based pricing for multimodal systems with heterogeneous users in an agent-based environment. *Transportation Research Part C: Emerging Technologies*, 62:133–148.

Zhong, R., Sumalee, A., Pan, T., and Lam, W. H. K., 2014. Optimal and robust strategies for freeway traffic management under demand and supply uncertainties: An overview and general theory. *Transportmetrica A*, 10(10):849–877.

Zhong, R., Chen, C., Chow, A. H. F., Pan, T., Yuan, F., and He, Z., 2016a. Automatic calibration of fundamental diagram for first-order macroscopic freeway traffic models. *Journal of Advanced Transportation*, 50(3):363–385.

Zhong, R., Yuan, F., Pan, T., Chow, A. H., Chen, C., and Yang, Z., 2016b. Linear complementarity system approach to macroscopic freeway traffic modelling: Uniqueness and convexity. *Transportmetrica A*, 12(2):142–174.

Zhong, R., Chen, C., Huang, Y., Sumalee, A., Lam, W., and Xu, D., 2017. Robust Perimeter Control for Two Urban Regions with Macroscopic Fundamental Diagrams: A Control-Lyapunov Function Approach. *Transportation Research Part B: Methodological*. doi: http://dx.doi.org/10.1016/j.trb.2017.09.008.